

EFFICIENT NUMERICAL METHOD FOR RELIABLE UPPER AND LOWER BOUNDS ON HOMOGENIZED PARAMETERS

LIYA GAYNUTDINOVA¹, MARTIN LADECKÝ^{1,2}, ALEŠ NEKVINDA¹, IVANA PULTAROVÁ¹
AND JAN ZEMAN^{2,3}

Abstract. A numerical procedure providing guaranteed two-sided bounds on the effective coefficients of elliptic partial differential operators is presented. The upper bounds are obtained in a standard manner through the variational formulation of the problem and by applying the finite element method. To obtain the lower bounds we formulate the dual variational problem and introduce appropriate approximation spaces employing the finite element method as well. We deal with the 3D setting, which has been rarely considered in the literature so far. The theoretical justification of the procedure is presented and supported with illustrative examples.

2020 Mathematics Subject Classification. 35B27, 65N15, 49N15, 65F10.

July 24, 2023.

1. INTRODUCTION

Composite materials are prominent in many areas of engineering because of their diverse useful properties. Such materials are often considered to possess a periodic structure. To obtain the effective properties of those materials, the homogenization theory [17, 27] was developed, and the recent decades witnessed a great progress of efficient numerical methods in homogenization. They developed from the iterative fixed point computational schemes for Lippmann-Schwinger equation using collocation principles [29, 30] to the finite difference or variational approaches which use Krylov subspace solvers and the fast Fourier transform algorithm to accelerate the convergence; see e.g. [4, 23, 25, 38, 39, 47] or [12, 26, 35] for recent comprehensive reviews. As a result of these developments, the contemporary FFT-accelerated solvers are capable of up-scaling complex multi-physics processes defined on high-resolution voxel microstructures on conventional hardware. Yet, the issues of convergence

Keywords and phrases: homogenization of linear elliptic PDEs; duality-based error estimates; finite element method; Helmholtz decomposition; conjugate gradient method

¹ Department of Mathematics, Faculty of Civil Engineering, Czech Technical University in Prague, Thákurova 2077/7, Prague, Czech Republic

² Department of Mechanics, Faculty of Civil Engineering, Czech Technical University in Prague, Thákurova 2077/7, Prague, Czech Republic

³ Corresponding author: jan.zeman@cvut.cz

and accuracy (or error estimates) of the resulting homogenized properties have gained attention only recently; see [36, 37, 46] for the current convergence results and [8] for a recent study on error estimation.

In this work, we adopt a duality-based framework, see e.g. [3, 41, 45], consider a 3D scalar elliptic partial differential equation with periodic data, and introduce a numerical procedure providing guaranteed and arbitrarily close upper and lower bounds on the homogenized data. Our approach rests on earlier results by Dvořák and Haslinger [6, 14] where, however, only a 2D setting is considered; see also [3]. The main difficulty of generalization to 3D consists in choosing appropriate finite dimensional approximation spaces to the periodic divergence-free solution space of the dual problems. The only paper dealing with a 3D setting is [44] where the approximation spaces are formed by smooth periodic spectral Fourier functions. There are two drawbacks of numerical computation with a truncated Fourier expansion. Numerical solutions of differential equations with discontinuous data may suffer from ringing artifacts, e.g. [24, Section 3] for examples in the present context, and computing the elements of stiffness matrices exactly may become difficult even for piecewise constant coefficients and grids fitted to coefficient jumps [28, 42]. However, computing elements of the linear system (almost) exactly is important for providing reliable bounds on the homogenized data.

In this paper we consider a cuboid domain $Y \subset \mathbb{R}^3$ and a symmetric matrix function $A \in L^\infty(Y, \mathbb{R}^{3 \times 3})$ which is uniformly positive definite a.e. in Y , i.e., there exist $c_1, c_2 > 0$ such that $c_1(v, v)_{\mathbb{R}^3} \leq (A(x)v, v)_{\mathbb{R}^3} \leq c_2(v, v)_{\mathbb{R}^3}$ for all $v \in \mathbb{R}^3$ and a.a. $x \in Y$. Here $(u, v)_{\mathbb{R}^3}$ denotes the inner product of vectors u and v of the Euclidean space \mathbb{R}^3 . The related homogenization problem [17] reads to find a homogenized data matrix $A^* \in \mathbb{R}^{3 \times 3}$ such that

$$(A^* \xi, \xi)_{\mathbb{R}^3} = \inf_{u \in H_{\text{per}}^1(Y, \mathbb{R})} \frac{1}{|Y|} \int_Y (A(\xi + \nabla u), \xi + \nabla u)_{\mathbb{R}^3} dx \quad (1)$$

for all $\xi \in \mathbb{R}^3$, where $|Y|$ denotes the volume of Y . Our goal in this paper is to present a method that yields guaranteed, feasible, and arbitrarily close upper and lower bounds on A^* . Let A_h^* be obtained as a result of a minimization problem (1) over only a finite-dimensional subspace $V_h \subset H_{\text{per}}^1(Y, \mathbb{R})$; see Section 2 for details and definitions. Matrix A_h^* is an upper bound to A^* , $A^* \preceq A_h^*$, in the sense that

$$(A^* \xi, \xi)_{\mathbb{R}^3} \leq (A_h^* \xi, \xi)_{\mathbb{R}^3} \quad \text{for all } \xi \in \mathbb{R}^3.$$

A sufficiently close approximation A_h^* to A^* can be obtained by appropriate refining of the solution space V_h . It remains to obtain the computable sufficiently accurate guaranteed lower bounds for A^* . This sets the goal of this paper.

The outline of the paper is as follows. In the next section we recall the Helmholtz decomposition of $L^2(Y, \mathbb{R}^3)$ into rotation-free and divergence-free Y -periodic functions. As the first result of this paper, we propose the approximation spaces for this decomposition based on the finite element (FE) discretization using standard Lagrange finite elements. In Section 3 we suggest and theoretically prove a tool for obtaining the lower bounds

on homogenized coefficients. In contrast to [6,44], we build the theoretical justification on a simple optimization result which is proved here, instead of on a rather involved perturbation-duality argument. At the end of the section, we propose a novel projection-based approximate solution of the dual problem and its error estimate. This solution does not involve any iterative solution process. The reader who searches for computational algorithms only may skip Sections 2 and 3 and proceed to Section 4 directly in which we comment on the implementation of our procedure and present some numerical examples. Some concluding remarks and the plans for further research are found in Section 5.

2. HELMHOLTZ DECOMPOSITION AND APPROXIMATION SPACES

We consider a cuboid domain $Y \subset \mathbb{R}^3$, $Y = (0, a_1) \times (0, a_2) \times (0, a_3)$, $a_j > 0$, $j = 1, 2, 3$. Then Y is Lipschitz, connected, and bounded. We only deal with Euclidean space \mathbb{R}^3 . Changing the setting to \mathbb{R}^2 is straightforward and fully described in [6].

2.1. Helmholtz decomposition of periodic fields

Let us recall for a domain $\Omega \subset \mathbb{R}^3$ the function space $L^2(\Omega, \mathbb{R}^k)$ of functions $u : \Omega \rightarrow \mathbb{R}^k$, $u = (u_1, \dots, u_k)^T$, with the inner product $(u, v) = \int_{\Omega} (u, v)_{\mathbb{R}^k} dx$, and the function space $L^1(\Omega, \mathbb{R}^k)$ containing functions $u : \Omega \rightarrow \mathbb{R}^k$ with finite Lebesgue integrals $\int_{\Omega} |u_j(x)| dx$, $j = 1, \dots, k$.

Considering the special case $\Omega = Y$, the Y -periodic extension u_{per} of $u \in L^1(Y, \mathbb{R}^k)$ is defined as

$$u_{\text{per}}(x) = u(x) \text{ for a.a. } x \in Y,$$

and

$$u_{\text{per}}(x) = u_{\text{per}}(x + (a_1, 0, 0)) = u_{\text{per}}(x + (0, a_2, 0)) = u_{\text{per}}(x + (0, 0, a_3)) \text{ for a.a. } x \in \mathbb{R}^3.$$

The mean value $\langle u \rangle \in \mathbb{R}^k$ of $u \in L^1(Y, \mathbb{R}^k)$ is defined as

$$\langle u \rangle = \frac{1}{|Y|} \int_Y u \, dx,$$

where $|Y| = a_1 a_2 a_3$. Any subspace of $L^1(Y, \mathbb{R}^k)$ of functions with zero mean is denoted by the subscript $_{\text{mean},0}$.

Let us introduce the function spaces

$$\begin{aligned} H^1(Y, \mathbb{R}^k) &= \{u \in L^2(Y, \mathbb{R}^k); \nabla u_j \in L^2(Y, \mathbb{R}^3), j = 1, \dots, k\} \\ H^{\text{curl}}(Y, \mathbb{R}^3) &= \{u \in L^2(Y, \mathbb{R}^3); \text{curl } u \in L^2(Y, \mathbb{R}^3)\} \\ H^{\text{div}}(Y, \mathbb{R}^3) &= \{u \in L^2(Y, \mathbb{R}^3); \text{div } u \in L^2(Y, \mathbb{R})\} \end{aligned}$$

where $u : Y \rightarrow \mathbb{R}$ and $v : Y \rightarrow \mathbb{R}^3$ and where the differential operators

$$\nabla u = \left(\frac{\partial}{\partial x_1}, \frac{\partial}{\partial x_2}, \frac{\partial}{\partial x_3} \right) u, \quad \operatorname{div} v = \nabla \cdot v, \quad \operatorname{curl} v = \nabla \times v$$

are defined in the weak sense. The functions with zero weak divergence in Y are defined as

$$H^{\operatorname{div},0}(Y, \mathbb{R}^3) = \left\{ u \in L^2(Y, \mathbb{R}^3); \int_Y u \cdot \nabla \phi \, dx = 0, \phi \in C_0^\infty(Y, \mathbb{R}) \right\},$$

see, e.g., [13]. Let the subscript loc denote that a required property is fulfilled on all compact subsets of \mathbb{R}^3 . Let us define

$$\begin{aligned} H_{\operatorname{per}}^1(Y, \mathbb{R}^k) &= \{u \in H^1(Y, \mathbb{R}^k); u_{\operatorname{per}} \in H_{\operatorname{loc}}^1(\mathbb{R}^3, \mathbb{R}^k)\} \\ H_{\operatorname{per}}^{\operatorname{div},0}(Y, \mathbb{R}^3) &= \{u \in H^{\operatorname{div},0}(Y, \mathbb{R}^3); u_{\operatorname{per}} \in H_{\operatorname{loc}}^{\operatorname{div},0}(\mathbb{R}^3, \mathbb{R}^3)\} \\ \nabla H_{\operatorname{per}}^1(Y, \mathbb{R}) &= \{u \in L^2(Y, \mathbb{R}^3); u = \nabla v, v \in H_{\operatorname{per}}^1(Y, \mathbb{R})\}. \end{aligned}$$

From [5, 34] or [40] and [17], we have the following theorem.

Theorem 2.1. *A vector field $u \in L^2(Y, \mathbb{R}^3)$ satisfies $\operatorname{div} u = 0$ if and only if there exists a vector potential $v \in H^{\operatorname{curl}}(Y, \mathbb{R}^3)$ for which $u = \operatorname{curl} v$.*

In our setting, we will decompose $L^2(Y, \mathbb{R}^3)$ into periodic irrotational (potential) fields ($\nabla H_{\operatorname{per}}^1(Y, \mathbb{R})$) and periodic divergence free ($H_{\operatorname{per}}^{\operatorname{div},0}(Y, \mathbb{R}^3)$) fields. Let us first recall the following divergence theorem [2, 13]:

Lemma 2.2. *There exists a continuous linear operator $\gamma : H^{\operatorname{div},0}(Y, \mathbb{R}^3) \rightarrow H^{-1/2}(\partial Y, \mathbb{R})$ such that*

$$\gamma u = u \cdot n|_{\partial Y} \quad \text{for } u \in C^\infty(\overline{Y}, \mathbb{R}^3).$$

For $u \in H^{\operatorname{div},0}(Y, \mathbb{R}^3)$ and $v \in H^1(Y, \mathbb{R})$ we have

$$\int_Y u \cdot \nabla v \, dx = \langle \gamma u, Tv \rangle, \tag{2}$$

where Tv is the trace of v on the boundary ∂Y and $\langle \phi, \psi \rangle$ is a duality pairing between $\psi \in H^{1/2}(\partial Y, \mathbb{R})$ and $\phi \in H^{-1/2}(\partial Y, \mathbb{R})$.

Remark 2.3. Images of γ defined by Lemma 2.2 can be denoted by $\gamma u = u \cdot n$ and called normal fluxes of $u \in H^{\operatorname{div},0}(Y, \mathbb{R}^3)$ on ∂Y .

It is well known, see e.g., [13], that for every function $u \in L^2(Y, \mathbb{R}^3)$ there exist functions v and w such that $u = \nabla v + \operatorname{curl} w$ where $v \in H^1(Y, \mathbb{R})$, $w \in H^1(Y, \mathbb{R}^3)$, and $\gamma(u - \nabla v) = 0$. In our approach, however, we will deal with Y -periodic functions only, which are less frequent in the literature. Although the main results needed later are stated in [17], we present their detailed derivation in Appendix A for the readers convenience.

Theorem 2.4. *Let us define*

$$W = \{u \in L^2(Y, \mathbb{R}^3); \int_Y u \cdot \nabla \phi \, dx = 0 \text{ for all } \phi \in H_{\text{per}}^1(Y, \mathbb{R})\}.$$

Then

$$W = H_{\text{per}}^{\text{div},0}(Y, \mathbb{R}^3).$$

Remark 2.5. The spaces $H_{\text{per}}^{\text{div},0}(Y, \mathbb{R}^3)$, $\nabla H_{\text{per}}^1(Y, \mathbb{R})$, and $H_{\text{per,mean},0}^{\text{div},0}(Y, \mathbb{R}^3)$ are closed subspaces of $L^2(Y, \mathbb{R}^3)$; the proof proceeds in the standard way using the Green theorem and the Cauchy-Schwartz inequality, see e.g. [13]. Then from Theorem 2.4 it follows that there is an $L^2(Y; \mathbb{R}^3)$ -orthogonal decomposition (the Helmholtz decomposition)

$$L^2(Y, \mathbb{R}^3) = H_{\text{per}}^{\text{div},0}(Y, \mathbb{R}^3) \oplus \nabla H_{\text{per}}^1(Y, \mathbb{R}). \quad (3)$$

Moreover, we have

$$L^2(Y, \mathbb{R}^3) = H_{\text{per,mean},0}^{\text{div},0}(Y, \mathbb{R}^3) \oplus \nabla H_{\text{per}}^1(Y, \mathbb{R}) \oplus \mathbb{R}^3.$$

2.2. Approximation spaces

As we will see in Section 3, for the numerical computation of the upper and lower bounds on A^* it is necessary to accurately approximate functions from $\nabla H_{\text{per}}^1(Y, \mathbb{R})$ and from $H_{\text{per}}^{\text{div},0}(Y, \mathbb{R}^3)$, respectively. A common approach to approximate functions of $\nabla H_{\text{per}}^1(Y, \mathbb{R})$ is to use the FE basis functions, also called shape functions and their derivatives. Approximation of functions of $H_{\text{per}}^{\text{div},0}(Y, \mathbb{R}^3)$ is less common. In the literature, they are also called statically admissible functions, e.g. [20], and special unisolvent FE spaces were proposed, e.g., [15, 32]. In the remaining part of this section, we show how standard FE basis functions can be used to approximate $H_{\text{per,mean},0}^{\text{div},0}(Y, \mathbb{R}^3)$. The absence of unisolvence is compensated by an easy implementation.

To this goal, let us define the following matrices

$$Q_1 = \begin{pmatrix} 0 & -1 & 0 \\ 1 & 0 & 0 \\ 0 & 0 & 0 \end{pmatrix}, \quad Q_2 = \begin{pmatrix} 0 & 0 & 1 \\ 0 & 0 & 0 \\ -1 & 0 & 0 \end{pmatrix} \quad \text{and} \quad Q_3 = \begin{pmatrix} 0 & 0 & 0 \\ 0 & 0 & -1 \\ 0 & 1 & 0 \end{pmatrix}. \quad (4)$$

Lemma 2.6. *The closure of*

$$W_Q = \text{span} (Q_1 \nabla H_{\text{per}}^1(Y, \mathbb{R}) \cup Q_2 \nabla H_{\text{per}}^1(Y, \mathbb{R}) \cup Q_3 \nabla H_{\text{per}}^1(Y, \mathbb{R})) \quad (5)$$

with respect to the metric of $L^2(Y, \mathbb{R}^3)$ equals to $H_{\text{per,mean},0}^{\text{div},0}(Y, \mathbb{R}^3)$.

Proof. Let $u \in W_Q$. Then there exist potentials ψ_1 , ψ_2 and ψ_3 in $H_{\text{per}}^1(Y, \mathbb{R})$ such that $u = Q_1 \nabla \psi_1 + Q_2 \nabla \psi_2 + Q_3 \nabla \psi_3$. Then for $\phi \in C_{\text{per}}^\infty(Y, \mathbb{R})$

$$\int_Y (Q_j \nabla \psi_j) \cdot \nabla \phi \, dx = - \int_Y \psi_j \cdot \text{div} Q_j^T \nabla \phi \, dx + \int_{\partial Y} (n \cdot Q_j^T \nabla \phi) \psi_j \, ds = 0, \quad j = 1, 2, 3,$$

because $\operatorname{div} Q_j^T \nabla \phi = 0$, and $(n \cdot Q_j^T \nabla \phi) \psi_j$ has opposite values on the opposite faces of Y . Then

$$\int_Y u \cdot \nabla \phi \, dx = \int_Y (Q_1 \nabla \psi_1 + Q_2 \nabla \psi_2 + Q_3 \nabla \psi_3) \cdot \nabla \phi \, dx = 0.$$

Since $C_{\text{per}}^\infty(Y, \mathbb{R})$ is dense in $H_{\text{per}}^1(Y, \mathbb{R})$, we get $u \in H_{\text{per}}^{\text{div},0}(Y, \mathbb{R}^3)$ by Theorem 2.4. Since ψ_j is periodic, $Q_j \nabla \psi_j$ is periodic as well and the mean of each component is zero. This yields that W_Q is a subspace of $H_{\text{per,mean},0}^{\text{div},0}(Y, \mathbb{R}^3)$. Since $H_{\text{per,mean},0}^{\text{div},0}(Y, \mathbb{R}^3)$ is closed, then it also contains the closure of W_Q .

Now consider $u \in H_{\text{per,mean},0}^{\text{div},0}(Y, \mathbb{R}^3)$. Because $H_{\text{per,mean},0}^{\text{div},0}(Y, \mathbb{R}^3) \subset L^2(Y, \mathbb{R}^3)$, the field u admits the Fourier series representation

$$u(x) = \sum_{j \in \mathbb{Z}^3, j \neq 0} u_j(x), \quad u_j(x) = c_j \exp(ij \cdot x), \quad c_j \in \mathbb{C}^3, \quad (6)$$

where we assumed, for notation simplicity, $Y = (0, 2\pi)^3$. Note that

$$\operatorname{div} u_j = i c_j \cdot j \exp(ij \cdot x)$$

where $j = (j_1, j_2, j_3)^T \in \mathbb{Z}^3$, $x = (x_1, x_2, x_3)^T \in Y$. Every term u_j of the expansion (6) is Y -periodic. Using $\operatorname{div} u = 0$ and Theorem 2.4 with $\phi = \exp(ij \cdot x)$, we get $j \cdot c_j = 0$ for all $j \in \mathbb{Z}^3$, which implies that each Fourier coefficient c_j must be of a form $c_j = t_j \times j$ with $t_j \in \mathbb{C}^3$. Therefore,

$$c_j = (t_{j,1} Q_1 + t_{j,2} Q_2 + t_{j,3} Q_3) j, \quad t_{j,1}, t_{j,2}, t_{j,3} \in \mathbb{C},$$

and we can write

$$u_j(x) = (t_{j,1} Q_1 + t_{j,2} Q_2 + t_{j,3} Q_3) \nabla \exp(ij \cdot x), \quad t_{j,1}, t_{j,2}, t_{j,3} \in \mathbb{C}. \quad (7)$$

Let us consider a sufficiently close (in the norm of $L^2(Y, \mathbb{R}^3)$) approximation $u^{(m)}$ to u with a finite number of terms

$$u^{(m)}(x) = \sum_{|j| \leq m} u_j(x) = \sum_{|j| \leq m} c_j \exp(ij \cdot x). \quad (8)$$

Then

$$u^{(m)}(x) = \sum_{|j| \leq m} c_j \exp(ij \cdot x) = \sum_{|j| \leq m} (t_{j,1} Q_1 + t_{j,2} Q_2 + t_{j,3} Q_3) \nabla \exp(ij \cdot x) = Q_1 \nabla \psi_1(x) + Q_2 \nabla \psi_2(x) + Q_3 \nabla \psi_3(x)$$

where

$$\psi_s(x) = \sum_{|j| \leq m} t_{j,s} \exp(ij \cdot x),$$

$\psi_s \in C_{\text{per}}^\infty(Y, \mathbb{R})$, $s = 1, 2, 3$. Such a $u^{(m)} \in W_Q$ can be arbitrarily close to u .

Considering general cell $Y = (0, a_1) \times (0, a_2) \times (0, a_3)$ yields

$$\operatorname{div} u_j = \frac{i}{2\pi} \sum_{k=1}^3 (c_j)_k a_k j_k \exp\left(\frac{i}{2\pi} \sum_{k=1}^3 a_k j_k x_k\right).$$

The coefficients of the field u with zero divergence are then

$$c_j = (t_{j,1}Q_1 + t_{j,2}Q_2 + t_{j,3}Q_3) a \odot j$$

where $a \odot j$ denotes the element-wise (Hadamard) product. Thus (7) remains valid, and the statement of the lemma as well. \square

Corollary 2.7. *From Lemma 2.6 it follows that the following orthogonal decomposition holds*

$$L^2(Y, \mathbb{R}^3) = \nabla H_{\text{per}}^1(Y, \mathbb{R}) \oplus \overline{W_Q} \oplus \mathbb{R}^3, \quad (9)$$

where

$$W_Q = \text{span} \left(Q_1 \nabla H_{\text{per}}^1(Y, \mathbb{R}) \cup Q_2 \nabla H_{\text{per}}^1(Y, \mathbb{R}) \cup Q_3 \nabla H_{\text{per}}^1(Y, \mathbb{R}) \right). \quad (10)$$

In analogy to the notation $\nabla H_{\text{per}}^1(Y, \mathbb{R})$, we can use the notation $W_Q = \text{curl } H_{\text{per}}^1(Y, \mathbb{R}^3)$ and write

$$L^2(Y, \mathbb{R}^3) = \nabla H_{\text{per}}^1(Y, \mathbb{R}) \oplus \text{curl } H_{\text{per}}^1(Y, \mathbb{R}^3) \oplus \mathbb{R}^3. \quad (11)$$

Remark 2.8. From density of standard FE spaces in $H_{\text{per}}^1(Y, \mathbb{R})$ (for example, continuous piece-wise linear periodic functions; see e.g. [1]) and from (9), we obtain that the set of gradients of the FE basis functions is dense in $\nabla H_{\text{per}}^1(Y, \mathbb{R})$ in the $L^2(Y, \mathbb{R}^3)$ metric, and the set of the same gradients multiplied by matrices Q_j , $j = 1, 2, 3$, is dense in $\text{curl } H_{\text{per}}^1(Y, \mathbb{R}^3)$ in the same metric. An interested reader may compare our approach with a related study [19] for non-periodic domains and different boundary conditions. As such, the presented approach extends and combines the two previous frameworks proposed in [6, 44]. Specifically, our characterization of the space $\text{curl } H_{\text{per}}^1(Y, \mathbb{R}^3)$ generalizes the two-dimensional stream function technique of Dvořák [6] to three dimensions. In [44], the same space was constructed from $L^2(Y, \mathbb{R}^3)$ using a projection operator with an explicit expression in the Fourier space. Note that the dimensions of the spaces spanned with the trigonometric and finite element bases coincide in both two and three dimensions.

3. UPPER AND LOWER BOUNDS ON HOMOGENIZED COEFFICIENTS

In this section, we focus on obtaining the upper and lower bounds on A^* , where A^* is defined by (1). By bounds, we mean symmetric positive definite matrices $C_1^*, C_2^* \in \mathbb{R}^{3 \times 3}$ such that

$$(C_1^* \xi, \xi)_{\mathbb{R}^3} \leq (A^* \xi, \xi)_{\mathbb{R}^3} \leq (C_2^* \xi, \xi)_{\mathbb{R}^3}, \quad \text{for all } \xi \in \mathbb{R}^3, \quad (12)$$

which we denote by $C_1^* \preceq A^* \preceq C_2^*$.

Recall that $A : Y \rightarrow \mathbb{R}^{3 \times 3}$ is uniformly positive definite and bounded a.e. in Y . It is well known that the minimum of quadratic functional defined by (1) is attained for $u = u_\xi$ satisfying

$$\int_Y (A \nabla u_\xi, \nabla v)_{\mathbb{R}^3} dx = - \int_Y (A \xi, \nabla v)_{\mathbb{R}^3} dx, \quad \text{for all } v \in H_{\text{per}}^1(Y; \mathbb{R}). \quad (13)$$

Observe that the mapping $\xi \rightarrow u_\xi$ is linear, which yields for all $\xi \in \mathbb{R}^3$,

$$\begin{aligned} (A^* \xi, \mu)_{\mathbb{R}^3} &= \frac{1}{2} ((A^*(\xi + \mu), \xi + \mu)_{\mathbb{R}^3} - (A^* \xi, \xi)_{\mathbb{R}^3} - (A^* \mu, \mu)_{\mathbb{R}^3}) \\ &= \frac{1}{|Y|} \int_Y (A(\xi + \nabla u_\xi), \mu + \nabla u_\mu)_{\mathbb{R}^3} dx. \end{aligned}$$

By (13) we also have

$$(A^* \xi, \mu)_{\mathbb{R}^3} = \frac{1}{|Y|} \int_Y (A(\xi + \nabla u_\xi), \mu)_{\mathbb{R}^3} dx = \frac{1}{|Y|} \int_Y (A \xi, \mu + \nabla u_\mu)_{\mathbb{R}^3} dx. \quad (14)$$

3.1. Upper bounds

The minimizing solution $u_\xi \in H_{\text{per}}^1(Y, \mathbb{R})$ in (1) is obtained by solving (13). A numerical solution can be found on a finite-dimensional subspace U_h of $H_{\text{per}}^1(Y, \mathbb{R})$, usually generated by FE functions. Since (1) is formulated as a variational problem where the minimum is to be reached over some infinite dimensional space, any minimum over a subspace $U_h \subset H_{\text{per}}^1(Y, \mathbb{R})$ or even any functions from $H_{\text{per}}^1(Y, \mathbb{R})$ yield an upper bound to A^* in the sense (12). More precisely, let $\tilde{u}^{(j)} \in U_h$ be arbitrary and $\xi = e^{(j)}$, $j = 1, 2, 3$, where $e^{(j)}$ is the j -th column of 3×3 identity matrix. Let

$$(A_h^*)_{jk} = \frac{1}{|Y|} \int_Y (A(e^{(k)} + \nabla \tilde{u}^{(k)}), e^{(j)} + \nabla \tilde{u}^{(j)})_{\mathbb{R}^3} dx, \quad j, k = 1, 2, 3.$$

Then A_h^* is an upper bound to A^* in the sense of (12), $A^* \preceq A_h^*$. A sufficiently close approximation can be obtained by refining the solution space U_h and thus by having $u^{(j)}$ closer to their minimizing counterparts in $H_{\text{per}}^1(Y, \mathbb{R})$ in general. It remains to obtain the computable sufficiently close guaranteed lower bounds, which is the goal of the next two subsections.

3.2. Lower bounds

Our estimation method relies on the perturbation duality theorem. Various forms of the theorem can be found in the literature; see e.g. [7, 15, 17]. To keep the paper self-contained, we present and prove a certain form of the duality theorem as Lemma B.1, which is significantly simpler than the version in [7] used in, e.g., [6, 44]. Using Lemma B.1, the problem (1) is then transformed to the dual one; see Lemma B.2. Both lemmas and their proofs are found in Appendix B.

We now formulate the duality principle for the homogenization problems. In the rest of this paper, we will use the following notation

$$\begin{aligned} H &= L^2(Y, \mathbb{R})^3, & H_0 &= \{u \in L^2(Y, \mathbb{R}^3), \langle u \rangle = 0\}, & U &= H_{\text{per}}^1(Y, \mathbb{R}), \\ V &= \nabla U, & W &= H_{\text{per}}^{\text{div},0}(Y, \mathbb{R}^3), & W_0 &= H_{\text{per,mean},0}^{\text{div},0}(Y, \mathbb{R}^3). \end{aligned}$$

Note that the mean $\langle v \rangle = 0$ for any $v \in V$. According to Remark 2.5 we have

$$H = V \oplus W \quad \text{and} \quad H_0 = V \oplus W_0.$$

Since V is a closed subspace in H , we can use minimum instead of infimum in (1).

Let us define *the dual problem* to (1): Find a matrix $B^* \in \mathbb{R}^{3 \times 3}$ such that for every $\alpha \in \mathbb{R}^3$

$$(B^* \alpha, \alpha)_{\mathbb{R}^3} = \frac{1}{|Y|} \min_{w \in W_0} \int_Y (A^{-1}(\alpha + w), \alpha + w)_{\mathbb{R}^3} dx. \quad (15)$$

Note that B^* is symmetric and positive definite.

Theorem 3.1. *Let B^* be defined by (15). Then we have*

$$(B^*)^{-1} = A^*.$$

Moreover, let $\alpha = A^* \xi$, $u_\xi \in U$ and $w_\alpha \in W_0$ be the minimizers in (1) and (15), respectively, and let w_1 be given by

$$A^* \xi + w_1 = A(\xi + \nabla u_\xi), \quad \xi \in \mathbb{R}^3. \quad (16)$$

Then $w_1 = w_\alpha$.

Following Theorem 3.1 we can get $A^* = (B^*)^{-1}$ by solving the dual problem (15). Since the dual problem is a variational minimization problem, for any approximate solution B_h^* we obtain an upper bound to B^* which provides a lower bound to A^* , $(B_h^*)^{-1} \preceq (B^*)^{-1} \preceq A^*$, e.g., [16, Corollary 7.7.4]. For completeness, we present this well-known equivalence:

Lemma 3.2. *Let $A, B \in \mathbb{R}^{n \times n}$ be symmetric positive definite matrices. Then*

$$v^T A v \leq v^T B v, \quad \text{for all } v \in \mathbb{R}^n \quad \iff \quad v^T B^{-1} v \leq v^T A^{-1} v, \quad \text{for all } v \in \mathbb{R}^n. \quad (17)$$

3.3. Numerical solution

Numerical solution of the minimizers $u_\xi \in U$ and $w_\alpha \in W_0$ of (1) and (15), respectively, usually yields some inexact $\tilde{u}_\xi \in U$ and $\tilde{w}_\alpha \in W_0$, respectively. Then obviously

$$\begin{aligned} (A^*\xi, \xi)_{\mathbb{R}^3} &\leq \frac{1}{|Y|} \int_Y (A(\xi + \tilde{u}_\xi), \xi + \nabla \tilde{u}_\xi)_{\mathbb{R}^3} dx \\ (B^*\alpha, \alpha)_{\mathbb{R}^3} &\leq \frac{1}{|Y|} \int_Y (A^{-1}(\alpha + \tilde{w}_\alpha), \alpha + \tilde{w}_\alpha)_{\mathbb{R}^3} dx. \end{aligned}$$

The difference between the left and right-hand sides is handled in the following lemma; see also [36, 46], in which $\lambda_1(A)$ and $\lambda_2(A)$ denote the essential infimum and the essential supremum of minimal and maximal eigenvalues of A over Y , respectively.

Lemma 3.3. *Let $\tilde{u}_\xi, \tilde{u}_\nu \in U$ and $\tilde{w}_\alpha, \tilde{w}_\beta \in W_0$ be some approximations to u_ξ, u_ν and w_α, w_β , respectively, for some $\xi, \nu, \alpha, \beta \in \mathbb{R}^3$. Then*

$$\begin{aligned} &\left| \int_Y (A(\xi + \nabla \tilde{u}_\xi), \nu + \nabla \tilde{u}_\nu)_{\mathbb{R}^3} dx - |Y|(A^*\xi, \nu)_{\mathbb{R}^3} \right| \\ &= \left| \int_Y (A(\nabla \tilde{u}_\xi - \nabla u_\xi), \nabla \tilde{u}_\nu - \nabla u_\nu)_{\mathbb{R}^3} dx \right| \leq \lambda_2(A) \|\tilde{u}_\xi - u_\xi\|_U \|\tilde{u}_\nu - u_\nu\|_U \\ &\left| \int_Y (A^{-1}(\alpha + \tilde{w}_\alpha), \beta + \tilde{w}_\beta)_{\mathbb{R}^3} dx - |Y|(B^*\alpha, \beta)_{\mathbb{R}^3} \right| \\ &= \left| \int_Y (A^{-1}(\tilde{w}_\alpha - w_\alpha), \tilde{w}_\beta - w_\beta)_{\mathbb{R}^3} dx \right| \leq \frac{1}{\lambda_1(A)} \|\tilde{w}_\alpha - w_\alpha\|_H \|\tilde{w}_\beta - w_\beta\|_H. \end{aligned}$$

Proof. We first deal with the primal problem. Note that for all $\xi \in \mathbb{R}^3$ and $v \in U$ we have

$$\int_Y (A(\xi + \nabla u_\xi), \nabla v) dx = 0.$$

Then

$$\begin{aligned} &\int_Y (A(\xi + \nabla \tilde{u}_\xi), \nu + \nabla \tilde{u}_\nu)_{\mathbb{R}^3} dx - |Y|(A^*\xi, \nu)_{\mathbb{R}^3} \\ &= \int_Y (A(\xi + \nabla \tilde{u}_\xi), \nu + \nabla \tilde{u}_\nu)_{\mathbb{R}^3} dx - \int_Y (A(\xi + \nabla u_\xi), \nu + \nabla u_\nu)_{\mathbb{R}^3} dx \\ &= \int_Y (A\xi, \nabla \tilde{u}_\nu)_{\mathbb{R}^3} + (A\nabla \tilde{u}_\xi, \nu)_{\mathbb{R}^3} + (A\nabla \tilde{u}_\xi, \nabla \tilde{u}_\nu)_{\mathbb{R}^3} - (A\nabla u_\xi, \nu)_{\mathbb{R}^3} dx \\ &= \int_Y -(A\nabla u_\xi, \nabla \tilde{u}_\nu)_{\mathbb{R}^3} - (A\nabla \tilde{u}_\xi, \nabla u_\nu)_{\mathbb{R}^3} + (A\nabla \tilde{u}_\xi, \nabla \tilde{u}_\nu)_{\mathbb{R}^3} + (A\nabla u_\xi, \nabla u_\nu)_{\mathbb{R}^3} dx \\ &= \int_Y (A(\nabla \tilde{u}_\xi - \nabla u_\xi), \nabla \tilde{u}_\nu - \nabla u_\nu)_{\mathbb{R}^3} dx. \end{aligned}$$

Absolute value of the last term is obviously bounded from above by $\lambda_2(A) \|\tilde{u}_\xi - u_\xi\|_U \|\tilde{u}_\nu - u_\nu\|_U$. The proof for the dual form is analogous. \square

Let us now assume that we use some finite-dimensional discretization space $U_h \subset U$. For $\xi \in \mathbb{R}^3$, $\|\xi\|_{\mathbb{R}^3} = 1$, we obtain $\tilde{u}_\xi \approx u_\xi$, $\tilde{u}_\xi \in U_h$. Let us assume that there exists $\delta_1 > 0$, such that $\|\tilde{u}_\xi - u_\xi\|_U \leq \delta_1$. Similarly, for two other vectors which together with ξ form an orthonormal basis of \mathbb{R}^3 , let us obtain approximations of all elements of A^* ; let us call such a matrix \tilde{A}^* and assume that

$$\|\tilde{A}^* - A^*\|_2 \leq \delta_2.$$

We now consider some discretization space $W_{0,h} \subset W_0$ and want to use (16) to obtain some $\tilde{w} \in W_{0,h}$ which would be relatively close to $w_{\tilde{\alpha}}$, where $\tilde{\alpha} = \tilde{A}^*\xi$. Let us denote

$$w_H = A(\xi + \nabla\tilde{u}_\xi) - \tilde{A}^*\xi.$$

The field $w_H \in H$ may not belong to $W_{0,h}$ (and even to W_0), because FE spaces, in general, are not endowed with the discrete Helmholtz decomposition, unlike, for example, discrete Fourier bases; see, e.g. [44]. Therefore, let $\tilde{w} \in W_{0,h}$ be obtained as the H -orthogonal projection of w_H onto $W_{0,h}$

$$(\tilde{w}, v)_H = (w_H, v)_H, \quad v \in W_{0,h}.$$

If Y is a cuboid and the grid is regular, this projection would be easy to obtain numerically using the fast discrete Fourier transform; see, e.g. [22]. Then the question remains what is the difference between \tilde{w} and $w_{\tilde{\alpha}} \in W_0$, the minimizer of (15) with $\alpha := \tilde{\alpha}$. According to Lemma 3.3, we would then immediately obtain the bound to the error of computing $(B^*\tilde{\alpha}, \tilde{\alpha})_{\mathbb{R}^3}$ by using \tilde{w} instead of the exact minimizer $w_{\tilde{\alpha}}$. As we will see in the next lemma, the rate of convergence for the lower bound of A^* obtained in this way is the same as for the upper bound.

Lemma 3.4. *Let $\xi \in \mathbb{R}^3$, $\|\xi\|_2 = 1$, be arbitrary. Let u_ξ be the minimizer in (1) and let $\tilde{u}_\xi \in U$ be such that $\|\tilde{u}_\xi - u_\xi\|_U < \delta_1$. Let $\tilde{A}^* \in \mathbb{R}^{3 \times 3}$ be an approximation to A^* such that $\|\tilde{A}^* - A^*\|_2 < \delta_2$. Denote $\tilde{\alpha} = \tilde{A}^*\xi$ and*

$$w_H = A\xi + A\nabla\tilde{u}_\xi - \tilde{A}^*\xi.$$

Let $\tilde{w} \in W_{0,h}$ be an H -orthogonal projection of w_H onto $W_{0,h}$, i.e.

$$(\tilde{w}, v)_H = (w_H, v)_H, \quad v \in W_{0,h}.$$

Then

$$\|\tilde{w} - w_{\tilde{\alpha}}\|_H \leq c_1\delta_1 + c_2\delta_2 + ch, \tag{18}$$

where $w_{\tilde{\alpha}} \in W_0$ is the exact minimizer in (15) for $\alpha := \tilde{\alpha}$, and $c_1, c_2, c > 0$ depend on $|Y|$ and on essentially extremal eigenvalues of A^ and A on Y .*

Proof. We first estimate $\|w_H - \tilde{w}\|_H$. Let us denote $d_H = w_H - \tilde{w}$. Since $d_H \in H$, due to the Helmholtz decomposition (3) (see also Corollary 2.7) we can decompose it into three pair-wise H -orthogonal parts, $d_H = d_W + d_V + d_C$ where $d_W \in W_0$, $d_V \in V$ and $d_C \in \mathbb{R}^3$. Therefore we have $\|d_H\|_H^2 = \|d_W\|_H^2 + \|d_V\|_H^2 + \|d_C\|_H^2$. Using (13) we have for all $v \in V$

$$\begin{aligned} (d_V, v)_H &= (w_H - \tilde{w}, v)_H = (A\xi + A\nabla\tilde{u}_\xi - \tilde{A}^*\xi - \tilde{w}, v)_H = (A\xi + A\nabla\tilde{u}_\xi, v)_H \\ &= (A\xi + A\nabla\tilde{u}_\xi - A\nabla u_\xi + A\nabla u_\xi, v)_H = (A(\nabla\tilde{u}_\xi - \nabla u_\xi), v)_H. \end{aligned}$$

Then

$$|(d_V, v)_H| \leq \lambda_2(A) \|\nabla\tilde{u}_\xi - \nabla u_\xi\|_H \|v\|_H \leq \lambda_2(A) \delta_1 \|v\|_H,$$

and thus $\|d_V\|_H \leq \lambda_2(A) \delta_1$. We now estimate $\|d_C\|_H$. Using (14), we have for all $\nu \in \mathbb{R}^3$

$$\begin{aligned} (d_C, \nu)_H &= (w_H - \tilde{w}, \nu)_H = (A\xi + A\nabla\tilde{u}_\xi - \tilde{A}^*\xi - \tilde{w}, \nu)_H = (A\xi + A\nabla\tilde{u}_\xi - \tilde{A}^*\xi, \nu)_H \\ &= (A\nabla\tilde{u}_\xi - \tilde{A}^*\xi - A\nabla u_\xi + A^*\xi, \nu)_H = (A\nabla\tilde{u}_\xi - A\nabla u_\xi, \nu)_H + |Y| \nu^T (A^* - \tilde{A}^*) \xi. \end{aligned}$$

Then

$$|(d_C, \nu)_H| \leq \lambda_2(A) |Y|^{\frac{1}{2}} \|\nabla\tilde{u}_\xi - \nabla u_\xi\|_H \|\nu\|_2 + \delta_2 |Y| \|\nu\|_2 \|\xi\|_2 \leq \delta_1 \lambda_2(A) |Y|^{\frac{1}{2}} \|\nu\|_2 + \delta_2 |Y| \|\nu\|_2$$

and thus $\|d_C\|_H \leq \delta_1 \lambda_2(A) |Y|^{\frac{1}{2}} + \delta_2 |Y|$. For the estimate of the distance d_W between the H -orthogonal projection of $w_H \in H$ onto W_h and its approximation $\tilde{w} \in W_{0,h}$ we obtain a standard inequality $\|d_W\|_H \leq ch$, where the real constant c does not depend on h ; see e.g. [1]. Now we estimate $\|w_H - w_{\tilde{\alpha}}\|_H$. Note that from (16) for any $\alpha \in \mathbb{R}^3$ the exact minimizer in (15) is

$$w_\alpha = A(A^*)^{-1}\alpha + A\nabla u_{(A^*)^{-1}\alpha} - \alpha.$$

Then setting $\alpha := \tilde{\alpha} = \tilde{A}^*\xi$ we have

$$\begin{aligned} \|w_H - w_{\tilde{\alpha}}\|_H &= \|A\xi + A\nabla\tilde{u}_\xi - \tilde{A}^*\xi - (A(A^*)^{-1}\tilde{\alpha} + A\nabla u_{(A^*)^{-1}\tilde{\alpha}} - \tilde{\alpha})\|_H \\ &= \|A\xi + A\nabla\tilde{u}_\xi - (A(A^*)^{-1}\tilde{A}^*\xi + A\nabla u_{(A^*)^{-1}\tilde{A}^*\xi})\|_H \\ &\leq \|A\xi - A(A^*)^{-1}\tilde{A}^*\xi\|_H + \|A(\nabla\tilde{u}_\xi - \nabla u_{(A^*)^{-1}\tilde{A}^*\xi})\|_H \\ &= \|A(A^*)^{-1}(A^* - \tilde{A}^*)\xi\|_H + \|A(\nabla\tilde{u}_\xi - \nabla u_\xi + \nabla u_\xi - \nabla u_{(A^*)^{-1}\tilde{A}^*\xi})\|_H \\ &\leq \frac{\lambda_2(A)}{\lambda_1(A^*)} |Y| \delta_2 + \lambda_2(A) \delta_1 + \|A(\nabla u_\xi - \nabla u_{(A^*)^{-1}\tilde{A}^*\xi})\|_H \\ &\leq \frac{\lambda_2(A)}{\lambda_1(A^*)} |Y| \delta_2 + \lambda_2(A) \delta_1 + \lambda_2(A)^{\frac{1}{2}} \|A^{1/2}(\nabla u_\xi - \nabla u_{(A^*)^{-1}\tilde{A}^*\xi})\|_H. \end{aligned}$$

Since the minimizers u_ξ in (1) depend on ξ linearly, then denoting $\nu = (A^*)^{-1}\tilde{A}^*\xi$ we have

$$\|A^{1/2}(\nabla u_\xi - \nabla u_{(A^*)^{-1}\tilde{A}^*\xi})\|_H^2 = \int_Y (A(\nabla u_\xi - \nabla u_\nu), \nabla u_\xi - \nabla u_\nu)_{\mathbb{R}^3} dx = |Y|(\xi - \nu)^T A^*(\xi - \nu).$$

We also have

$$\xi - (A^*)^{-1}\tilde{A}^*\xi = (A^*)^{-1}(A^* - \tilde{A}^*)\xi.$$

Then

$$\|w_H - w_{\tilde{\alpha}}\|_H \leq \frac{\lambda_2(A)|Y|}{\lambda_1(A^*)}\delta_2 + \lambda_2(A)\delta_1 + \frac{\lambda_2(A)^{\frac{1}{2}}|Y|^{\frac{1}{2}}}{\lambda_1(A^*)^{\frac{1}{2}}}\delta_2,$$

and finally,

$$\|\tilde{w} - w_{\tilde{\alpha}}\|_H \leq \|\tilde{w} - w_H\|_H + \|w_H - w_{\tilde{\alpha}}\|_H \leq c_1\delta_1 + c_2\delta_2 + ch,$$

where $c_1, c_2 > 0$ depend on extremal eigenvalues of A and A^* , and c is provided by approximation properties of $W_{0,h}$ in W_0 . \square

4. NUMERICAL EXAMPLES AND IMPLEMENTATION REMARKS

This section is devoted to the practical computation of the bounds on A^* . In the first part, we suggest a procedure for getting the upper and lower bounds on A^* . In the second part, we go into detail and discuss some implementation aspects and present some numerical examples.

4.1. Algorithm

The algorithm for providing two-sided bounds on A^* is as follows:

Algorithm 1. Computing A_h^* and B_h^* .

1. Choose a FE discretization and solve (1) with $\xi = e^{(j)}$, and get the solutions $u^{(j)} \in U$, $j = 1, 2, 3$.
Set $(A_h^*)_{jk} = \frac{1}{|Y|} \int_Y (A(e^{(k)} + \nabla u^{(k)}), e^{(j)} + \nabla u^{(j)})_{\mathbb{R}^3} dx$.
2. Choose a FE discretization and solve (15) with $\alpha = e^{(j)}$, and get the solutions $w^{(j)} \in W_0$, $j = 1, 2, 3$.
Set $(B_h^*)_{jk} = \frac{1}{|Y|} \int_Y (A^{-1}(e^{(k)} + w^{(k)}), e^{(j)} + w^{(j)})_{\mathbb{R}^3} dx$.
3. The bounds on the true A^* are $(B_h^*)^{-1} \preceq A^* \preceq A_h^*$.

Remark 4.1. (a) The choices of the FEM settings in steps 1 and 2 in Algorithm 1 to get B_h^* and A_h^* , respectively, are independent.

- (b) Matrices $(B_h^*)^{-1}$ and A_h^* are the lower and upper bounds, respectively, to A^* , only if the system matrices and the right-hand side vectors are evaluated exactly. In practice, this means that the elements of the system matrices must be integrated exactly; otherwise, the bounds are not guaranteed anymore. On the other hand, the solutions $u^{(j)}$ and $w^{(j)}$ do not have to be exact solutions of the discretized systems; they only have to belong to the respective function spaces, i.e. $u^{(j)} \in U$ and $w^{(j)} \in W_0$, $j = 1, 2, 3$.

- (c) Taking any basis $\{\xi^{(1)}, \xi^{(2)}, \xi^{(3)}\}$ of \mathbb{R}^3 and defining A_h^* using any functions $u^{(1)}, u^{(2)}, u^{(3)} \in U$ in (1) yields $A^* \preceq A_h^*$. The closest upper bound is, however, obtained by such $u^{(j)}$, $j = 1, 2, 3$, that minimize (1). An analogous statement holds for the lower bounds.

In practical computation, instead of solving (15) for a given $\alpha \in \mathbb{R}^3$ in some subspace of W_0 , we can use formula (16) in Theorem 3.1 to get a good approximation \tilde{w} of its minimizing field $w_\alpha \in W_0$ and thus to get an approximation \tilde{B}_h^* of B^* ,

$$(\tilde{B}_h^* \alpha, \alpha)_{\mathbb{R}^3} = \frac{1}{|Y|} \int_Y (A^{-1}(\alpha + \tilde{w}), \alpha + \tilde{w})_{\mathbb{R}^3} dx. \quad (19)$$

In practice, we cannot use $w_1 = A(\xi + \nabla u_\xi) - A^* \xi$ as \tilde{w} directly, because we know neither u_ξ nor A^* exactly. Instead, we must only consider some approximations of these quantities \tilde{u}_ξ and \tilde{A}^* , respectively, obtained from step 1 of Algorithm 1, and then set

$$w_H = A(\xi + \nabla \tilde{u}_\xi) - \tilde{A}^* \xi \in H. \quad (20)$$

Such a w_H , however, may not belong to W_0 in general. Therefore, we compute a projection \tilde{w} of w_H onto some finite-dimensional space $W_{0,h} \subset W_0$. In this paper, we propose to use the orthogonal projection on a FE space $W_{0,h} \subset W_0$. The orthogonality is understood in the sense of $H = L^2(Y, \mathbb{R}^3)$ inner product. Then $\tilde{w} \in W_{0,h}$ is obtained as a solution of

$$(\tilde{w}, v)_H = (w_H, v)_H, \quad v \in W_{0,h}. \quad (21)$$

and \tilde{B}_h^* is then obtained from (19) where we set $\alpha := \tilde{\alpha} = \tilde{A}^* \xi$. Since \tilde{w} is not the minimizer of (15) with $\tilde{\alpha} = \tilde{A}^* \xi$, we have

$$(B_h^* \tilde{\alpha}, \tilde{\alpha})_{\mathbb{R}^3} \leq (\tilde{B}_h^* \tilde{\alpha}, \tilde{\alpha})_{\mathbb{R}^3}. \quad (22)$$

In section 3.3 we prove that the approximations A_h^* and $(\tilde{B}_h^*)^{-1}$ of the exact matrix A^* as its upper and lower bounds, respectively, are asymptotically of the same rate. We can also consider any other kind of projection, such as energy-like inner product projections. In our numerical experiments, the simplest one (21) gives good numerical results; thus, we do not involve the others in our consideration. It is important to emphasize that due to periodic boundary conditions and using uniform grids, the linear system matrix is block circulant, and thus the solution of (21) can be obtained by the fast discrete Fourier transform without solving any system of linear equations.

Algorithm 2. Computing \tilde{B}_h^* from approximate solutions of the primal problem.

1. Using Algorithm 1, step 1, for $\xi = e^{(j)} \in \mathbb{R}^3$ get (possibly inexact) solutions $\tilde{u}^{(j)} \in U$, $j = 1, 2, 3$, and an approximation \tilde{A}^* to $A^* \in \mathbb{R}^{3 \times 3}$.
2. For $j = 1, 2, 3$:
set $w_H^{(j)} = A(e^{(j)} + \nabla \tilde{u}^{(j)}) - \tilde{A}^* e^{(j)}$

find $\tilde{w}^{(j)} \in W_{0,h}$ such that $(\tilde{w}^{(j)}, v)_H = (w_H^{(j)}, v)_H$, for all $v \in W_{0,h}$
 set $\alpha^{(j)} = \tilde{A}^* e^{(j)}$

3. Build \tilde{B}_h^* such that $(\tilde{B}_h^* \alpha^{(k)}, \alpha^{(j)})_{\mathbb{R}^3} = \frac{1}{|Y|} \int_Y (A^{-1}(\alpha^{(k)} + \tilde{w}^{(k)}), \alpha^{(j)} + \tilde{w}^{(j)})_{\mathbb{R}^3} dx$.

Due to the regular grid of Y and periodic boundary conditions, the mass matrix of the linear system arising in (21) is block circulant, which enables using the discrete fast Fourier transform to obtain the solution without solving any system of linear equations.

4.2. Numerical examples

In our numerical experiments, we choose $a_i = 2\pi$, $i = 1, 2, 3$ and consider $N_{\text{vox}} = N_1 N_2 N_3$ voxels in Y . Each voxel is split into six tetrahedral elements of the same volume, thus the number of elements is $N_{\text{ele}} = 6N_{\text{vox}}$. We use continuous piece-wise linear Lagrange FE basis functions. To better pronounce the properties of the algebraic objects involved in our computation and/or to obtain insight into a matrix-free form of the algorithms, we can (in the spirit of e.g. [22]) construct the stiffness matrices and the right-hand side vectors from the so-called derivative matrices and from the coefficients in the following way. We build derivative matrices D_j , $j = 1, 2, 3$, which map the vector of nodal values of the basis function ϕ_m to the values of derivatives in quadrature points x^q (centers of elements), $(D_j)_{km} = \frac{\partial \phi_m}{\partial x_j}(x_k^q)$, $k = 1, \dots, N_{\text{ele}}$, $m = 1, \dots, N_{\text{vox}}$, $j = 1, 2, 3$. Following (4), we denote

$$D_{\text{grad}} = \begin{pmatrix} D_1 \\ D_2 \\ D_3 \end{pmatrix}, \quad D_{\text{curl}} = \begin{pmatrix} 0 & D_3 & -D_2 \\ -D_3 & 0 & D_1 \\ D_2 & -D_1 & 0 \end{pmatrix}, \quad (23)$$

i.e., $D_{\text{curl}} = (Q_3 D_{\text{grad}}, Q_2 D_{\text{grad}}, Q_1 D_{\text{grad}})$. The stiffness matrices and the right-hand sides of the discretized primal and dual problems (1) and (15), respectively, are

$$K = D_{\text{grad}}^T A D_{\text{grad}}, \quad \mathbf{b} = -D_{\text{grad}}^T A \mathbf{e}^\xi, \quad K_{\text{dual}} = D_{\text{curl}}^T A_{\text{inv}} D_{\text{curl}}, \quad \mathbf{b}_{\text{dual}} = -D_{\text{curl}}^T A_{\text{inv}} \mathbf{e}^\alpha,$$

where $A \in \mathbb{R}^{3N_{\text{ele}} \times 3N_{\text{ele}}}$ is composed from 3×3 blocks which are $N_{\text{ele}} \times N_{\text{ele}}$ diagonal matrices with the elements of $A(x_k^q) \in \mathbb{R}^{3 \times 3}$ as k -th elements of all respective nine diagonals. Similarly, $A_{\text{inv}} \in \mathbb{R}^{3N_{\text{ele}} \times 3N_{\text{ele}}}$ involves the elements of $(A(x_k^q))^{-1} \in \mathbb{R}^{3 \times 3}$. Vectors $\mathbf{e}^\xi, \mathbf{e}^\alpha \in \mathbb{R}^{3N_{\text{ele}}}$ contain repeating elements of ξ or α , respectively. Specifically, $\mathbf{e}^\xi = \text{kron}(\xi, \mathbf{1})$ or $\mathbf{e}^\alpha = \text{kron}(\alpha, \mathbf{1})$ when we consider ξ in (1) or α in (15), respectively, where kron denotes the Kronecker product and $\mathbf{1} = (1, \dots, 1)^T \in \mathbb{R}^{N_{\text{ele}}}$.

After obtaining the solutions \mathbf{u} of $K\mathbf{u} = \mathbf{b}$ and \mathbf{w} of $K_{\text{dual}}\mathbf{w} = \mathbf{b}_{\text{dual}}$, the approximate homogenized matrices follow from

$$\xi^T A_h^* \xi = (D_{\text{grad}} \mathbf{u} + \mathbf{e}^\xi)^T A (D_{\text{grad}} \mathbf{u} + \mathbf{e}^\xi) \quad (24)$$

$$\alpha^T B_h^* \alpha = (D_{\text{curl}} \mathbf{w} + \mathbf{e}^\alpha)^T A_{\text{inv}} (D_{\text{curl}} \mathbf{w} + \mathbf{e}^\alpha), \quad (25)$$

for arbitrary ξ and α in \mathbb{R}^3 .

Remark 4.2 (Dual systems). The dimension of the stiffness matrix K_{dual} for getting the lower bound is $3N_{\text{vox}}$ in contrast to the dimension N_{vox} of the stiffness matrix K of the primal problem (for getting the upper bound).

For both experiments, we set $N_1 = N_2 = N_3$ and consider the positive definite matrices A that are piecewise constant functions. Furthermore, the discretization is chosen such that A is constant on each element. Then the numerical quadrature rule with one quadrature point per element yields that the stiffness matrices and the right-hand side vectors are computed exactly. The tetrahedra in the mesh are oriented such that only the vertices $(0, 0, 0)$ and $(1, 1, 1)$ are connected by edges of the tetrahedra with seven other vertices, while the remaining vertices are connected each with four other vertices. The CG algorithm was stopped when the residual of the initial guess $x = 0$ was reduced by the factor 10^{-9} . All results can be reproduced using codes available in a Zenodo repository [9].

Example 1. For the first example, we consider the coefficients in the form

$$A(x) = \begin{pmatrix} 7 + \text{sign}(s_1 s_2) & -2 - \text{sign}(s_2 s_3) & \text{sign}(s_1 s_2 s_3) \\ -2 - \text{sign}(s_2 s_3) & 4.01 + \text{sign}(s_1 s_2) & 0 \\ \text{sign}(s_1 s_2 s_3) & 0 & 3 + \text{sign}(s_2 s_3) \end{pmatrix}, \quad x \in Y, \quad s_j = \sin\left(\frac{3}{2}x_j\right). \quad (26)$$

The data collected in Table 1 validate the upper-lower structure of the bounds, $(\tilde{B}_h^*)^{-1} \preceq (B_h^*)^{-1} \preceq A_h^*$, as follows from the positive definiteness of the differences $A_h^* - (B_h^*)^{-1}$ and $\tilde{B}_h^* - B_h^*$, and the monotone convergence of the diagonal elements upon the mesh refinement. We notice that for the primal problem, the number of CG iterations doubles with doubling the number of voxels per cell edge. Because of the expanded solution space, recall Remark 4.2, the dual problem needs substantially more iterations to converge as the number of iterations increases four times under the mesh refinement. The lower bound determined from the projected solution $(\tilde{B}_h^*)^{-1}$, on the other hand, provides an excellent approximation at a negligible computational cost. Additionally, we observe that the accuracy of the bounds surpasses the values reported for the Fourier basis in [42, 44]; even rather coarse discretization of $N_1 = N_2 = N_3 = 24$ yields the relative difference between upper and lower bounds less than 1%; see also [43] for a related study for the primal problem. This result is encouraging for the target applications in computational micromechanics of heterogeneous materials.

Figure 1 provides further insights into the behavior of the elements of upper-lower bounds matrices with an increasing number of degrees of freedom. Indeed, these extended data confirm the convergence of all the elements preserving the ordering $(\tilde{B}_h^*)^{-1} \preceq (B_h^*)^{-1} \preceq A_h^*$, with analogous ordering for all diagonal elements as a consequence. Figure 1 additionally certifies the quality of the projection-based lower bound $(\tilde{B}_h^*)^{-1}$ and the extra computational cost of the lower bound $(B_h^*)^{-1}$ that is reflected in its horizontal shift relative to the upper bound A_h^* .

Finally, we examine the rate of convergence of the homogenized properties by plotting the elements of the error estimates $(A_h^* - (B_h^*)^{-1})$ and $(A_h^* - (\tilde{B}_h^*)^{-1})$ against the number of voxels per edge $N_1 = N_2 = N_3$ in the

$N_1 = N_2 = N_3 = 6$								
$(\tilde{B}_h^*)^{-1}$			$(B_h^*)^{-1}$			A_h^*		
6.5702	-2.1432	-0.0629	6.6193	-2.1350	-0.0562	6.9126	-2.0937	-0.0114
-2.1432	3.8983	-0.0096	-2.1350	3.9140	-0.0064	-2.0937	4.0453	-0.0029
-0.0629	-0.0096	2.7496	-0.0562	-0.0064	2.7756	-0.0114	-0.0029	2.9602
			90	89	89	36	35	36

$$\text{eig}(A_h^* - (B_h^*)^{-1}) = (0.1205, 0.1707, 0.3181), \quad \text{eig}((B_h^*)^{-1} - (\tilde{B}_h^*)^{-1}) = (0.0135, 0.0243, 0.0528)$$

$N_1 = N_2 = N_3 = 12$								
$(\tilde{B}_h^*)^{-1}$			$(B_h^*)^{-1}$			A_h^*		
6.7067	-2.1203	-0.0471	6.7239	-2.1171	-0.0437	6.8414	-2.1012	-0.0253
-2.1203	3.9621	-0.0083	-2.1171	3.9675	-0.0073	-2.1012	4.0189	-0.0051
-0.0471	-0.0083	2.8249	-0.0437	-0.0073	2.8367	-0.0253	-0.0051	2.9105
			361	360	364	74	73	75

$$\text{eig}(A_h^* - (B_h^*)^{-1}) = (0.0475, 0.0677, 0.1275), \quad \text{eig}((B_h^*)^{-1} - (\tilde{B}_h^*)^{-1}) = (0.0047, 0.0102, 0.0197)$$

$N_1 = N_2 = N_3 = 24$								
$(\tilde{B}_h^*)^{-1}$			$(B_h^*)^{-1}$			A_h^*		
6.7625	-2.1117	-0.0390	6.7683	-2.1106	-0.0378	6.8091	-2.1049	-0.0314
-2.1117	3.9867	-0.0073	-2.1106	3.9885	-0.0070	-2.1049	4.0063	-0.0060
-0.0390	-0.0073	2.8594	-0.0378	-0.0070	2.8636	-0.0314	-0.0060	2.8891
			1,404	1,398	1,410	158	156	157

$$\text{eig}(A_h^* - (B_h^*)^{-1}) = (0.0164, 0.0234, 0.0444), \quad \text{eig}((B_h^*)^{-1} - (\tilde{B}_h^*)^{-1}) = (0.0015, 0.0036, 0.0066)$$

TABLE 1. Bounds on and estimates of the diagonal and off-diagonal elements, respectively, of the homogenized matrix A^* for coefficients specified in Example 1, Eq. (26). A_h^* and $(B_h^*)^{-1}$ denote the upper and lower bounds determined according to relations (24) and (25), and $(\tilde{B}_h^*)^{-1}$ is the lower bound determined from the projected solution (21). N_j , for $j = 1, 2, 3$, stands for the number of voxels per edge length, and the bottom rows collect the number of iterations of the conjugate gradient (CG) method, noting that computing $(\tilde{B}_h^*)^{-1}$ does not involve any CG iterations.

double-logarithmic scale in Figure 2. The results confirm the asymptotic scaling of $N_1^{-2} \approx h^2$, consistently with the results of Lemma 3.3 and the approximation property of piecewise linear basis functions, e.g., [1] (for the estimate $(A_h^* - (B_h^*)^{-1})$) and the additional results of Lemma 3.4 (for $(A_h^* - (\tilde{B}_h^*)^{-1})$). Note that the quadratic rate of convergence corresponds to the fact that the discontinuities in the coefficient $A(x)$ from Eq. (26) are exactly captured with the finite element mesh. The general case of discontinuity-unfitted meshes, typical of voxel-based geometries, corresponds to the linear convergence rate in homogenized properties; see [36, 46] for further discussion.

Example 2. To verify that the conclusions drawn from Example 1 also hold for other types of problem data, we perform an analogous analysis for the following coefficients:

$$A(x) = (2 + \text{sign}(s_1 s_2 s_3))I, \quad x = (x_1, x_2, x_3)^T \in Y, \quad s_j = \sin\left(\frac{3}{2}x_j\right) \quad (27)$$

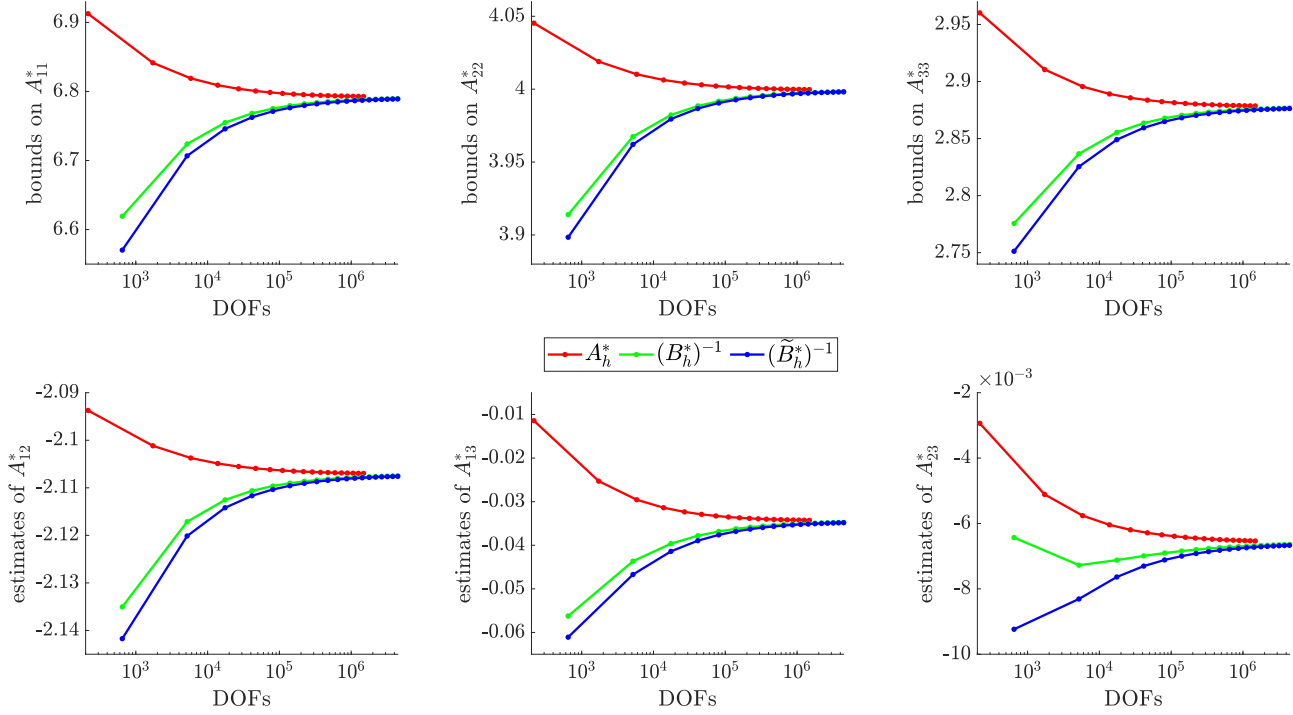


FIGURE 1. Estimates of elements of A^* for Example 1, Eq. (26). First row: Guaranteed upper and lower bounds on diagonal elements of A^* obtained as the respective diagonal elements of A_h^* , B_h^* and \tilde{B}_h^* . Second row: Analogously obtained estimates (not guaranteed bounds) for off-diagonal elements A_{12}^* , A_{13}^* , and A_{23}^* . Matrices A_h^* and B_h^* are computed according to Algorithm 1; matrices \tilde{B}_h^* are computed according to Algorithm 2. The horizontal axes denote the total number of degrees of freedom (DOFs) for every problem.

The results on the upper-lower bounds for discretizations $N_1 = N_2 = N_3 = 6, 12$, and 24 , collected in Table 2, confirm identical behavior as reported for Example 1 in Table 1. Similarly, the convergence graphs exhibit a similar pattern, although they are omitted here for brevity. Notice that the isotropy of local coefficients and the symmetry of their spatial distribution visible from Eq. (27) imply that the off-diagonal elements of the effective matrix A^* are zero. In contrast, the corresponding values of both matrices A_h^* and B_h^* are non-positive. Therefore, they estimate the exact value rather than bounding it.

5. CONCLUSIONS

We have presented a reliable numerical procedure for computing the guaranteed upper and lower bounds on a homogenized coefficient matrix defined by the cell problem (1). While the upper bound naturally follows from solving (1) approximately, e.g. on a finite-dimensional subspace of $H_{\text{per}}^1(Y, \mathbb{R})$, the lower bound requires building conforming approximations of the dual problem defined on $H_{\text{per}}^{\text{div},0}(Y, \mathbb{R}^3)$.

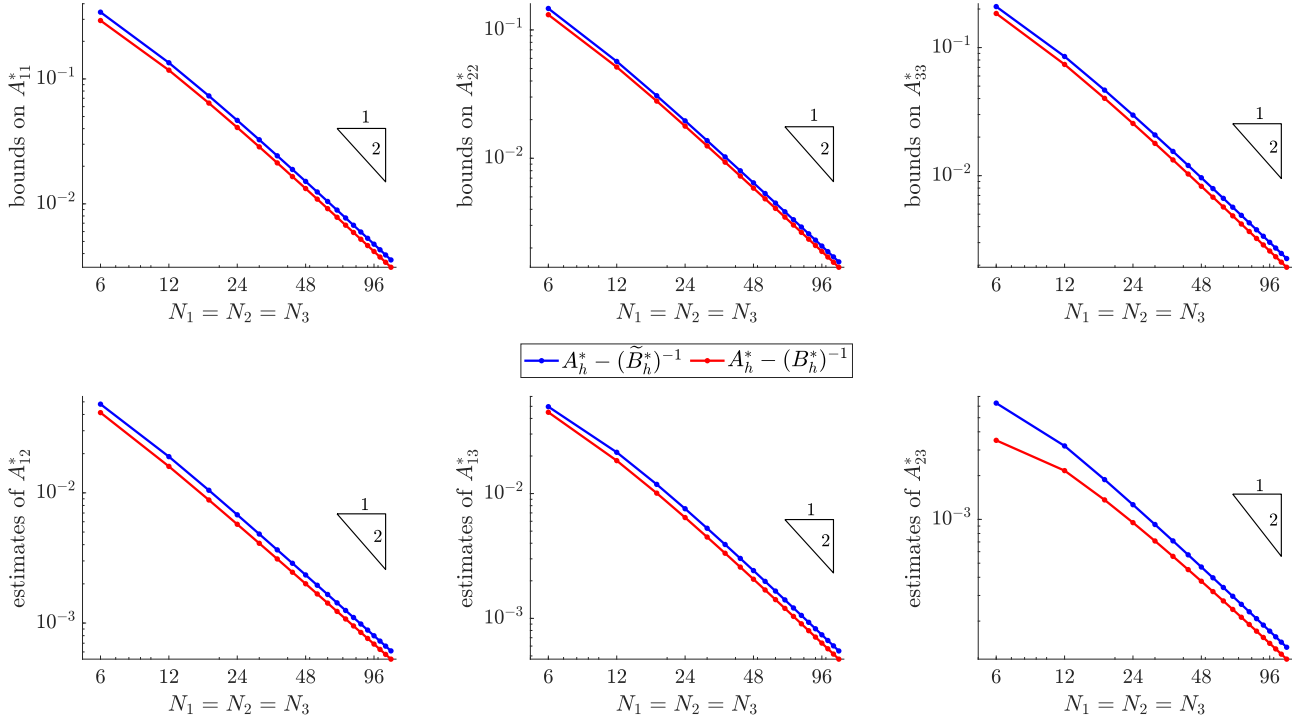


FIGURE 2. Convergence rates for the error estimates of the homogenized properties for coefficients of Example 1, Eq. (26). First row: Guaranteed error bounds on diagonal elements; second row: Estimates (not guaranteed bounds) on off-diagonal elements. N_j , $j = 1, 2, 3$ stands for the number of voxels per cell Y edge, and the triangle indicates the quadratic convergence rate with the size h , i.e., $h^2 \approx N_1^{-2}$.

Let us note that an efficient numerical method can be rarely developed without employing all relevant sources of the problem, starting from the physical meaning and formulation, through the choice of approximation spaces up to the numerical solution method and appropriate preconditioning; see a more involved exposition in [31]. Therefore, we presented most of this path here within our suggestion on the estimation method by proving the dual problem (Lemma B.2 and 3.1) based on a simple optimization result (Lemma B.1). We showed the Helmholtz decomposition of periodic fields and introduced another representation of $H_{\text{per}}^{\text{div},0}(Y, \mathbb{R}^3)$ (Lemma 2.6) which led to approximation spaces based on FE discretization. The lower bounds were then obtained by the numerical solution of (15).

Since the dual problem (15) is more computationally demanding than the primal one, it can be worth finding some good approximation of the minimizer of (15). We show how such a minimizer can be obtained using just a projection evaluated by the discrete fast Fourier transform.

Our next research will focus on efficient preconditioner for the problem (15), building on recent developments in the Laplace preconditioning of the primal problem [10, 11, 21, 33], to mitigate the dependence of the number

$N_1 = N_2 = N_3 = 6$								
$(\tilde{B}_h^*)^{-1}$			$(B_h^*)^{-1}$			A_h^*		
1.7035	-0.0043	-0.0043	1.7066	-0.0043	-0.0043	1.9446	-0.0016	-0.0016
-0.0043	1.7035	-0.0043	-0.0043	1.7066	-0.0043	-0.0016	1.9446	-0.0016
-0.0043	-0.0043	1.7035	-0.0043	-0.0043	1.7066	-0.0016	-0.0016	1.9446
			65	65	65	28	28	28

$$\text{eig}(A_h^* - (B_h^*)^{-1}) = (0.2353, 0.2353, 0.2434), \quad \text{eig}((B_h^*)^{-1} - (\tilde{B}_h^*)^{-1}) = (0.0030, 0.0031, 0.0031)$$

$N_1 = N_2 = N_3 = 12$								
$(\tilde{B}_h^*)^{-1}$			$(B_h^*)^{-1}$			A_h^*		
1.7831	-0.0023	-0.0023	1.7859	-0.0022	-0.0022	1.8938	-0.0002	-0.0002
-0.0023	1.7831	-0.0023	-0.0022	1.7859	-0.0022	-0.0002	1.8938	-0.0002
-0.0023	-0.0023	1.7831	-0.0022	-0.0022	1.7859	-0.0002	-0.0002	1.8938
			252	252	252	65	65	65

$$\text{eig}(A_h^* - (B_h^*)^{-1}) = (0.1059, 0.1059, 0.1119), \quad \text{eig}((B_h^*)^{-1} - (\tilde{B}_h^*)^{-1}) = (0.0028, 0.0028, 0.0029)$$

$N_1 = N_2 = N_3 = 24$								
$(\tilde{B}_h^*)^{-1}$			$(B_h^*)^{-1}$			A_h^*		
1.8214	-0.0008	-0.0008	1.8231	-0.0008	-0.0008	1.8671	-0.0000	-0.0000
-0.0008	1.8214	-0.0008	-0.0008	1.8231	-0.0008	-0.0000	1.8671	-0.0000
-0.0008	-0.0008	1.8214	-0.0008	-0.0008	1.8231	-0.0000	-0.0000	1.8671
			974	974	974	131	131	131

$$\text{eig}(A_h^* - (B_h^*)^{-1}) = (0.0433, 0.0433, 0.0456), \quad \text{eig}((B_h^*)^{-1} - (\tilde{B}_h^*)^{-1}) = (0.0017, 0.0017, 0.0017)$$

TABLE 2. Bounds on and estimates of the diagonal and off-diagonal elements, respectively, of the homogenized matrix A^* for coefficients specified in Example 2, Eq. (27). A_h^* and $(B_h^*)^{-1}$ denote the upper and lower bounds determined according to relations (24) and (25), and $(\tilde{B}_h^*)^{-1}$ is the lower bound determined from the projected solution (21). N_j , for $j = 1, 2, 3$, stands for the number of voxels per edge length, and the bottom rows collect the number of iterations of the conjugate gradient (CG) method, noting that computing $(\tilde{B}_h^*)^{-1}$ does not involve any CG iterations.

of iterations to convergence on spatial discretization (recall Tables 1 and 2), and on obtaining the two-sided bounds on more involved problems in elasticity.

The authors thank Michal Křížek (Institute of Mathematics, Czech Academy of Sciences) for valuable discussions and both anonymous referees for insightful and helpful comments. All authors acknowledge funding by the European Regional Development Fund (Centre of Advanced Applied Sciences – CAAS, CZ 02.1.01/0.0/0.0/16.019/0000778), by the Czech Science Foundation (projects No. 20-14736S (ML), and project No. 22-35755K (LG)), the Student Grant Competition of the Czech Technical University in Prague (project No. SGS23/002/OHK1/1T/11 (LG)).

REFERENCES

- [1] S. C. Brenner and L. R. Scott, *The Mathematical Theory of Finite Element Methods*, third ed., Texts in Applied Mathematics, vol. 15, Springer New York, NY, 2008, doi:10.1007/978-0-387-75934-0.
- [2] F. Brezzi and M. Fortin, *Mixed and Hybrid Finite Element Methods*, Springer Series in Computational Mathematics, vol. 15, Springer New York, NY, 1991, doi:10.1007/978-1-4612-3172-1.
- [3] M. Briane and D. Manceau, *Duality results in the homogenization of two-dimensional high-contrast conductivities*, Networks and Heterogeneous Media **3** (2008), no. 3, 509–522, doi:10.3934/nhm.2008.3.509.

- [4] S. Brisard and L. Dormieux, *FFT-based methods for the mechanics of composites: A general variational framework*, Computational Materials Science **49** (2010), no. 3, 663–671, doi:10.1016/j.commatsci.2010.06.009.
- [5] E. Deriaz and V. Perrier, *Orthogonal Helmholtz decomposition in arbitrary dimension using divergence-free and curl-free wavelets*, Applied and Computational Harmonic Analysis **26** (2009), no. 2, 249–269, doi:10.1016/j.acha.2008.06.001.
- [6] J. Dvořák, *A reliable numerical method for computing homogenized coefficients*, Tech. Report 0045, Charles University, Faculty of Mathematics and Physics, Prague, 1995, URL: <https://citeseerx.ist.psu.edu/doc/10.1.1.45.1190>.
- [7] I. Ekeland and R. Témam, *Convex analysis and variational problems*, Classics in Applied Mathematics, vol. 28, Society for Industrial and Applied Mathematics, Philadelphia, 1999, doi:10.1137/1.9781611971088.
- [8] R. Ferrier and C. Bellis, *A posteriori error estimations and convergence criteria in fast Fourier transform-based computational homogenization*, International Journal for Numerical Methods in Engineering **124** (2023), no. 4, 834–863, doi:<https://doi.org/10.1002/nme.7145>.
- [9] L. Gaynutdinova, M. Ladecký, A. Nekvinda, I. Pultarová, and J. Zeman, *Supplementary codes and datasets for "efficient numerical method for reliable upper and lower bounds on homogenized parameters"*, 2023, doi:10.5281/zenodo.8171432.
- [10] T. Gergelits, K. A. Mardal, B. F. Nielsen, and Z. Strakoš, *Laplacian preconditioning of elliptic PDEs: Localization of the eigenvalues of the discretized operator*, SIAM Journal on Numerical Analysis **57** (2019), no. 3, 1369–1394, doi:10.1137/18M1212458.
- [11] T. Gergelits, B. F. Nielsen, and Z. Strakoš, *Generalized spectrum of second order differential operators*, SIAM Journal on Numerical Analysis **58** (2020), no. 4, 2193–2211, doi:10.1137/20M1316159.
- [12] C. Gierden, J. Kochmann, J. Waimann, B. Svendsen, and S. Reese, *A review of FE-FFT-based two-scale methods for computational modeling of microstructure evolution and macroscopic material behavior*, Archives of Computational Methods in Engineering **1** (2022), 1–21, doi:10.1007/s11831-022-09735-6.
- [13] V. Girault and P.A. Raviart, *Finite Element Approximation of the Navier-Stokes Equations*, Lecture Notes in Mathematics, vol. 749, Springer Berlin, Heidelberg, 1979, doi:10.1007/BFb0063447.
- [14] J. Haslinger and J. Dvořák, *Optimum composite material design*, ESAIM: Mathematical Modelling and Numerical Analysis **29** (1995), no. 6, 657–686, doi:10.1051/M2AN/1995290606571.
- [15] J. Haslinger and I. Hlaváček, *Convergence of a finite element method based on the dual variational formulation*, Applications of Mathematics **21** (1976), no. 1, 43–65, doi:10.21136/am.1976.103621.
- [16] R.A. Horn and C.R. Johnson, *Matrix analysis*, second ed., Cambridge University Press, 2012, doi:10.1017/CB09781139020411.
- [17] V. V. Jikov, S. M. Kozlov, and O. A. Oleinik, *Homogenization of Differential Operators and Integral Functionals*, Springer Berlin Heidelberg, 1994, doi:10.1007/978-3-642-84659-5.
- [18] A. Kufner, S. Fučík, and O. John, *Function Spaces*, Noordhoff, Leyden; Academia, Prague, 1977.
- [19] M. Křížek and P. Neittaanmäki, *Internal FE approximation of spaces of divergence-free functions in three-dimensional domains*, International Journal for Numerical Methods in Fluids **6** (1986), no. 11, 811–817, doi:10.1002/FLD.1650061104.
- [20] M. Křížek, *Conforming equilibrium finite element methods for some elliptic plane problems*, RAIRO. Analyse numérique **17** (1983), no. 1, 35–65, doi:10.1051/M2AN/1983170100351.
- [21] M. Ladecký, I. Pultarová, and J. Zeman, *Guaranteed two-sided bounds on all eigenvalues of preconditioned diffusion and elasticity problems solved by the Finite Element method*, Applications of Mathematics **66** (2021), no. 1, 21–42, arXiv:2001.03673, doi:10.21136/AM.2020.0217-19.
- [22] M. Ladecký, R. J. Leute, A. Falsafi, I. Pultarová, L. Pastewka, T. Junge, and J. Zeman, *An optimal preconditioned FFT-accelerated finite element solver for homogenization*, Applied Mathematics and Computation **446** (2023), 127835, doi:10.1016/j.amc.2023.127835.
- [23] M. Leuschner and F. Fritzen, *Fourier-Accelerated Nodal Solvers (FANS) for homogenization problems*, Computational Mechanics **62** (2018), no. 3, 359–392, doi:10.1007/s00466-017-1501-5.
- [24] R. J. Leute, M. Ladecký, A. Falsafi, I. Jödicke, I. Pultarová, J. Zeman, T. Junge, and L. Pastewka, *Elimination of ringing artifacts by finite-element projection in FFT-based homogenization*, Journal of Computational Physics **453** (2022), 110931, doi:10.1016/j.jcp.2021.110931.
- [25] S. Lucarini and J. Segurado, *DBFFT: A displacement based FFT approach for non-linear homogenization of the mechanical behavior*, International Journal of Engineering Science **144** (2019), 103131, doi:10.1016/j.ijengsci.2019.103131.
- [26] S. Lucarini, M. V. Upadhyay, and J. Segurado, *FFT based approaches in micromechanics: Fundamentals, methods and applications*, Modelling and Simulation in Materials Science and Engineering **30** (2022), no. 2, 023002, doi:10.1088/1361-651x/ac34e1.
- [27] J. C. Michel, H. Moulinec, and P. Suquet, *Effective properties of composite materials with periodic microstructure: A computational approach*, Computer Methods in Applied Mechanics and Engineering **172** (1999), no. 1-4, 109–143, doi:10.1016/S0045-7825(98)00227-8.
- [28] V. Monchiet, *Combining FFT methods and standard variational principles to compute bounds and estimates for the properties of elastic composites*, Computer Methods in Applied Mechanics and Engineering **283** (2015), 454–473, doi:10.1016/j.cma.2014.10.005.

- [29] H. Moulinec and P. Suquet, *A fast numerical method for computing the linear and nonlinear mechanical properties of composites*, Comptes Rendus de l'Académie des sciences. Série II. Mécanique, physique, chimie, astronomie **318** (1994), no. 11, 1417–1423, URL: <https://hal.archives-ouvertes.fr/hal-03019226>.
- [30] ———, *A numerical method for computing the overall response of nonlinear composites with complex microstructure*, Computer Methods in Applied Mechanics and Engineering **157** (1998), no. 1-2, 69–94, [arXiv:2012.08962](https://arxiv.org/abs/2012.08962), [doi:10.1016/S0045-7825\(97\)00218-1](https://doi.org/10.1016/S0045-7825(97)00218-1).
- [31] J. Málek and Z. Strakoš, *Preconditioning and the Conjugate Gradient Method in the Context of Solving PDEs*, SIAM spotlights, vol. 1, Society for Industrial and Applied Mathematics, 2015, [doi:10.1137/1.9781611973846](https://doi.org/10.1137/1.9781611973846).
- [32] J. C. Nedelec, *Mixed finite elements in \mathbb{R}^3* , Numerische Mathematik **35** (1980), no. 3, 315–341, [doi:10.1007/BF01396415](https://doi.org/10.1007/BF01396415).
- [33] I. Pultarová and M. Ladecký, *Two-sided guaranteed bounds to individual eigenvalues of preconditioned finite element and finite difference problems*, Numerical Linear Algebra with Applications **28** (2021), no. 5, e2382, [doi:10.1002/NLA.2382](https://doi.org/10.1002/NLA.2382).
- [34] H. Ranocha, K. Ostaszewski, and P. Heinisch, *Discrete vector calculus and Helmholtz Hodge decomposition for classical finite difference summation by parts operators*, Communications on Applied Mathematics and Computation **2** (2020), no. 4, 581–611, [doi:10.1007/s42967-019-00057-2](https://doi.org/10.1007/s42967-019-00057-2).
- [35] M. Schneider, *A review of nonlinear FFT-based computational homogenization methods*, Acta Mechanica **232** (2021), no. 6, 2051–2100, [doi:10.1007/S00707-021-02962-1](https://doi.org/10.1007/S00707-021-02962-1).
- [36] ———, *Superaccurate effective elastic moduli via postprocessing in computational homogenization*, International Journal for Numerical Methods in Engineering **123** (2022), 4119–4135, [doi:10.1002/nme.7002](https://doi.org/10.1002/nme.7002).
- [37] ———, *On the effectiveness of the Moulinec–Suquet discretization for composite materials*, International Journal for Numerical Methods in Engineering **124** (2023), no. 14, [doi:https://doi.org/10.1002/nme.7244](https://doi.org/10.1002/nme.7244).
- [38] M. Schneider, D. Merkert, and M. Kabel, *FFT-based homogenization for microstructures discretized by linear hexahedral elements*, International Journal for Numerical Methods in Engineering **109** (2017), no. 10, 1461–1489, [doi:10.1002/nme.5336](https://doi.org/10.1002/nme.5336).
- [39] M. Schneider, F. Ospald, and M. Kabel, *Computational homogenization of elasticity on a staggered grid*, International Journal for Numerical Methods in Engineering **105** (2016), no. 9, 693–720, [doi:10.1002/nme.5008](https://doi.org/10.1002/nme.5008).
- [40] B. Schweizer, *On Friedrichs inequality, Helmholtz decomposition, vector potentials, and the div-curl lemma*, Springer INdAM Series, vol. 27, Springer International Publishing, 2018, pp. 65–79, [doi:10.1007/978-3-319-75940-1_4](https://doi.org/10.1007/978-3-319-75940-1_4).
- [41] H. Serrano, *Homogenization of quadratic complementary energies: A duality example*, Mathematica Bohemica **136** (2011), no. 2, 165–173, [doi:10.21136/mb.2011.141579](https://doi.org/10.21136/mb.2011.141579).
- [42] J. Vondřejc, *Improved guaranteed computable bounds on homogenized properties of periodic media by the Fourier-Galerkin method with exact integration*, International Journal for Numerical Methods in Engineering **107** (2016), no. 13, 1106–1135, [doi:10.1002/nme.5199](https://doi.org/10.1002/nme.5199).
- [43] J. Vondřejc and T. W.J. de Geus, *Energy-based comparison between the Fourier–Galerkin method and the finite element method*, Journal of Computational and Applied Mathematics **374** (2020), 112585, [doi:10.1016/j.cam.2019.112585](https://doi.org/10.1016/j.cam.2019.112585).
- [44] J. Vondřejc, J. Zeman, and I. Marek, *Guaranteed upper-lower bounds on homogenized properties by FFT-based Galerkin method*, Computer Methods in Applied Mechanics and Engineering **297** (2015), 258–291, [doi:10.1016/j.cma.2015.09.003](https://doi.org/10.1016/j.cma.2015.09.003).
- [45] Z. Wiecekowski, *Dual finite element methods in homogenization for elastic-plastic fibrous composite material*, International Journal of Plasticity **16** (2000), no. 2, 199–221, [doi:10.1016/S0749-6419\(99\)00070-4](https://doi.org/10.1016/S0749-6419(99)00070-4).
- [46] C. Ye and E.T. Chung, *Convergence of trigonometric and finite-difference discretization schemes for FFT-based computational micromechanics*, BIT Numerical Mathematics **63** (2023), no. 11, [doi:10.1007/s10543-023-00950-6](https://doi.org/10.1007/s10543-023-00950-6).
- [47] J. Zeman, J. Vondřejc, J. Novák, and I. Marek, *Accelerating a FFT-based solver for numerical homogenization of periodic media by conjugate gradients*, Journal of Computational Physics **229** (2010), no. 21, 8065–8071, [doi:10.1016/j.jcp.2010.07.010](https://doi.org/10.1016/j.jcp.2010.07.010).

APPENDIX A. PROOF OF THEOREM 2.4

Let us first introduce some auxiliary propositions. Given $M \subset \mathbb{R}^3$, $c \in \mathbb{R}^3$ and $b \in \mathbb{R}$, let us use the notation $c + bM = \{c + bx; x \in M\}$ and recall that $Y = (0, a_1) \times (0, a_2) \times (0, a_3)$.

Lemma A.1. *Let $u \in L^2(Y, \mathbb{R}^3)$. Then for all Y -periodic $\phi \in C^\infty(\mathbb{R}^3, \mathbb{R})$ and $c \in \mathbb{R}^3$ we have*

$$\int_Y u \cdot \nabla \phi \, dx = \int_{c+Y} u_{\text{per}} \cdot \nabla \phi \, dx.$$

Proof. Let us take first $c = (c_1, 0, 0)$ where $c_1 = ka_1 + b_1$, $k \in \mathbb{Z}$ and $|b_1| < a_1$. Denoting $b = (b_1, 0, 0)$ we have

$$\begin{aligned} \int_{c+Y} u_{\text{per}} \cdot \nabla \phi \, dx &= \int_{b+Y} u_{\text{per}} \cdot \nabla \phi \, dx = \int_{(b+Y) \cap Y} u \cdot \nabla \phi \, dx + \int_{(b+Y) \setminus Y} u_{\text{per}} \cdot \nabla \phi \, dx \\ &= \int_{Y \cap (b+Y)} u \cdot \nabla \phi \, dx + \int_{Y \setminus (b+Y)} u \cdot \nabla \phi \, dx = \int_Y u \cdot \nabla \phi \, dx. \end{aligned}$$

Then for $c = (c_1, c_2, c_3) \in \mathbb{R}^3$

$$\int_{c+Y} u_{\text{per}} \cdot \nabla \phi \, dx = \int_{(0, c_2, c_3) + Y} u_{\text{per}} \cdot \nabla \phi \, dx = \int_{(0, 0, c_3) + Y} u_{\text{per}} \cdot \nabla \phi \, dx = \int_Y u_{\text{per}} \cdot \nabla \phi \, dx = \int_Y u \cdot \nabla \phi \, dx.$$

□

Lemma A.2. Let $u \in L^2(Y, \mathbb{R}^3)$. Assume that for all Y -periodic $\phi \in C^\infty(\mathbb{R}^3, \mathbb{R})$

$$\int_Y u \cdot \nabla \phi \, dx = 0.$$

Then for all $c = (c_1, c_2, c_3) \in \mathbb{R}^3$ and $\psi \in C_0^\infty(c + Y, \mathbb{R})$

$$\int_{c+Y} u_{\text{per}} \cdot \nabla \psi \, dx = 0.$$

Proof. Extend ψ periodically to \mathbb{R}^3 and denote the extension by ψ_{per} . By Lemma A.1 we have

$$\int_{c+Y} u_{\text{per}} \cdot \nabla \psi \, dx = \int_{c+Y} u_{\text{per}} \cdot \nabla \psi_{\text{per}} \, dx = \int_Y u \cdot \nabla \psi_{\text{per}} \, dx = 0.$$

□

Lemma A.3. Let $u \in L^2(Y, \mathbb{R}^3)$. Assume that for all Y -periodic $\phi \in C^\infty(\mathbb{R}^3, \mathbb{R})$

$$\int_Y u \cdot \nabla \phi \, dx = 0.$$

Then for all $\psi \in C_0^\infty(\mathbb{R}^3, \mathbb{R})$ we have

$$\int_{\mathbb{R}^3} u_{\text{per}} \cdot \nabla \psi \, dx = 0.$$

Proof. Take any $\psi \in C_0^\infty(\mathbb{R}^3, \mathbb{R})$. Since $\text{supp } \psi$ is compact, there exists $m \in \mathbb{N}$ such that $\text{supp } \psi \subset \prod_{i=1}^3 [-ma_i, ma_i]$.

For $k \in \mathbb{R}^3$, let us use the notation $|k| = \max(|k_i|, i = 1, 2, 3)$. Let us denote for $k, j \in \mathbb{Z}^3$

$$\begin{aligned} Y_k &= (k_1 a_1, k_2 a_2, k_3 a_3) + Y, \\ Y_{k,j} &= \left(\left(k_1 + \frac{j_1}{2} \right) a_1, \left(k_2 + \frac{j_2}{2} \right) a_2, \left(k_3 + \frac{j_3}{2} \right) a_3 \right) + Y. \end{aligned}$$

Note that $\text{supp } \psi \subset \cup_{|k| \leq m+1} \bar{Y}_k$ and $\bar{Y}_k \subset \cup_{|j| \leq 1} Y_{k,j}$. Thus, the system $Y_{k,j}$, $|k| \leq m+1$, $|j| \leq 1$, is a finite open covering of $\text{supp } \psi$. Let us consider a partition of unity (see Theorem 5.3.8 in [18]) $\varphi_{k,j}$, $|k| \leq m+1$, $|j| \leq 1$, fulfilling: $\varphi_{k,j} \in C^\infty(\mathbb{R}^3, \mathbb{R})$, $\text{supp } \varphi_{k,j} \subset Y_{k,j}$, and $\sum_{|k| \leq m+1, |j| \leq 1} \varphi_{k,j}(x) = 1$ for all $x \in \text{supp } \psi$. Set $\psi_{k,j}(x) = \psi(x)\varphi_{k,j}(x)$, $x \in \mathbb{R}^3$. Then $\psi_{k,j} \in C_0^\infty(\mathbb{R}^3, \mathbb{R})$, $\text{supp } \psi_{k,j} \subset \bar{Y}_{k,j} \cap \text{supp } \psi$, and

$$\psi(x) = \sum_{|k| \leq m+1, |j| \leq 1} \psi_{k,j}(x), \quad x \in \text{supp } \psi.$$

Now we can write by Lemma A.2

$$\int_{\mathbb{R}^3} u_{\text{per}} \cdot \nabla \psi \, dx = \int_{\text{supp } \psi} u_{\text{per}} \cdot \sum_{|k| \leq m+1, |j| \leq 1} \nabla \psi_{k,j} \, dx = \sum_{|k| \leq m+1, |j| \leq 1} \int_{\bar{Y}_{k,j}} u_{\text{per}} \cdot \nabla \psi_{k,j} \, dx = 0.$$

□

Proof of Theorem 2.4:

Proof. Let us prove $H_{\text{per}}^{\text{div},0}(Y, \mathbb{R}^3) \subset W$ first. Let us have $u \in H_{\text{per}}^{\text{div},0}(Y, \mathbb{R}^3)$ and $\phi \in H_{\text{per}}^1(Y, \mathbb{R})$. Then using Lemma 2.2

$$\int_Y u \cdot \nabla \phi \, dx = \int_{\partial Y} (u \cdot n) \phi \, ds = 0,$$

because the normal fluxes $u \cdot n$ have opposite signs on any pair of opposite sides of Y , while ϕ has the same traces there. To prove $W \subset H_{\text{per}}^{\text{div},0}(Y, \mathbb{R}^3)$, consider $u \in W$. Since $C_0^\infty(Y, \mathbb{R}) \subset H_{\text{per}}^1(Y, \mathbb{R})$, we get

$$\int_Y u \cdot \nabla \phi \, dx = 0$$

for all $\phi \in C_0^\infty(Y, \mathbb{R})$, and thus $u \in H^{\text{div},0}(Y, \mathbb{R}^3)$. It remains to prove that u is Y -periodic, i.e. $u_{\text{per}} \in H_{\text{loc}}^{\text{div},0}(\mathbb{R}^3, \mathbb{R}^3)$. For $u \in W$ and $\psi \in C_0^\infty(\mathbb{R}^3, \mathbb{R})$, we get from Lemma A.3

$$\int_{\mathbb{R}^3} u_{\text{per}} \cdot \nabla \psi \, dx = 0.$$

□

APPENDIX B. PROOF OF THEOREM 3.1

Lemma B.1. *Let H be a real Hilbert space with the inner product (\cdot, \cdot) and let $H = V \oplus W$ where V and W are nontrivial closed subspaces of H and for all $v \in V$ and $w \in W$ it holds $(v, w) = 0$. Let F be a quadratic functional on H defined by*

$$F(u) = (A(u - u_0), u - u_0)$$

where $A : H \rightarrow H$ is a symmetric positive definite operator and $u_0 \in H$ and fixed. Then

$$\min_{v \in V} F(v) = \max_{w \in W} \left(\min_{u \in H} (F(u) - (w, u)) \right).$$

Proof. We prove " \geq " first. We have for all $w \in W$

$$\begin{aligned} \min_{v \in V} (F(v) - (w, v)) &\geq \min_{u \in H} (F(u) - (w, u)) \\ \min_{v \in V} F(v) &\geq \min_{u \in H} (F(u) - (w, u)) \end{aligned}$$

where we use $(v, w) = 0$ for $v \in V$ and $w \in W$. Thus

$$\min_{v \in V} F(v) \geq \max_{w \in W} \left(\min_{u \in H} (F(u) - (w, u)) \right).$$

To prove " \leq " let us first note that the minimum of $F(v)$ in V is achieved for such $v_0 \in V$ that

$$(Av_0 - Au_0, v) = 0, \quad \text{for all } v \in V. \quad (\text{b.1})$$

Then using (b.1) for $v = v_0$ we get

$$\min_{v \in V} F(v) = F(v_0) = (A(v_0 - u_0), v_0 - u_0) = (Au_0, u_0) - (Av_0, v_0). \quad (\text{b.2})$$

Let us take $w_0 = 2A(v_0 - u_0)$. From (b.1) we have $w_0 \in W$. We have

$$\begin{aligned} F(u) - (w_0, u) &= (A(u - u_0), u - u_0) - 2(Av_0 - Au_0, u) \\ &= (A(u - v_0), u - v_0) + (Au_0, u_0) - (Av_0, v_0). \end{aligned}$$

Clearly, the minimum of $F(u) - (w_0, u)$ in H is obtained for $u = v_0$, and then

$$\min_{u \in H} (F(u) - (w_0, u)) = (Au_0, u_0) - (Av_0, v_0),$$

which is equal to (b.2). This proves " \leq ". □

Lemma B.2. *Let $\xi \in \mathbb{R}^3$ be arbitrary and fixed. Let*

$$(A^*\xi, \xi)_{\mathbb{R}^3} = \frac{1}{|Y|} \min_{u \in U} \int_Y (A(\xi + \nabla u), \xi + \nabla u)_{\mathbb{R}^3} dx.$$

Then we have

$$(A^*\xi, \xi)_{\mathbb{R}^3} = \frac{1}{|Y|} \max_{w \in W} \int_Y -(A^{-1}w, w)_{\mathbb{R}^3} + 2(w, \xi)_{\mathbb{R}^3} dx.$$

Proof. Let $\xi \in \mathbb{R}^3$ be fixed. Let us define

$$F(v) = \frac{1}{2} \int_Y (A(\xi + v), \xi + v)_{\mathbb{R}^3} dx, \quad v \in V.$$

Then from Lemma B.1 we get

$$\begin{aligned}
\frac{|Y|}{2}(A^*\xi, \xi)_{\mathbb{R}^3} &= \min_{v \in V} F(v) = \max_{w \in W} \left(\min_{u \in H} (F(u) - (w, u)_H) \right) \\
&= \max_{w \in W} \left(\min_{u \in H} \left(\int_Y \frac{1}{2} (A(\xi + u), \xi + u)_{\mathbb{R}^3} dx - \int_Y (w, u)_{\mathbb{R}^3} dx \right) \right) \\
&= \max_{w \in W} \left(\min_{u \in H} \int_Y \frac{1}{2} (A(\xi + u), \xi + u)_{\mathbb{R}^3} - (w, u)_{\mathbb{R}^3} dx \right).
\end{aligned}$$

For any $w \in W$ the minimum is attained when $u = -\xi + A^{-1}w$ a.e. in Y . Then

$$\frac{|Y|}{2}(A^*\xi, \xi)_{\mathbb{R}^3} = \max_{w \in W} \left(\int_Y -\frac{1}{2} (A^{-1}w, w)_{\mathbb{R}^3} + (w, \xi)_{\mathbb{R}^3} dx \right).$$

□

Proof of Theorem 3.1:

Proof. Let $\xi \in \mathbb{R}^3$ be arbitrary and let $w \in W$ be split into $w = \beta + v$, $v \in W_0$, $\beta \in \mathbb{R}^3$. From Lemma B.2 and the definition (15) we have

$$\begin{aligned}
(A^*\xi, \xi)_{\mathbb{R}^3} &= \frac{1}{|Y|} \max_{w \in W} 2 \int_Y (w, \xi)_{\mathbb{R}^3} dx - \int_Y (A^{-1}w, w)_{\mathbb{R}^3} dx \\
&= \frac{1}{|Y|} \max_{v \in W_0, \beta \in \mathbb{R}^3} 2 \int_Y (\beta + v, \xi)_{\mathbb{R}^3} dx - \int_Y (A^{-1}(\beta + v), \beta + v)_{\mathbb{R}^3} dx \\
&= \frac{1}{|Y|} \max_{v \in W_0, \beta \in \mathbb{R}^3} 2 \int_Y (\beta, \xi)_{\mathbb{R}^3} dx - \int_Y (A^{-1}(\beta + v), \beta + v)_{\mathbb{R}^3} dx \\
&= \frac{1}{|Y|} \max_{\beta \in \mathbb{R}^3} \left(2 \int_Y (\beta, \xi)_{\mathbb{R}^3} dx - \min_{v \in W_0} \int_Y (A^{-1}(\beta + v), \beta + v)_{\mathbb{R}^3} dx \right) \\
&= \max_{\beta \in \mathbb{R}^3} \left(\frac{2}{|Y|} \int_Y (\beta, \xi)_{\mathbb{R}^3} dx - (B^*\beta, \beta)_{\mathbb{R}^3} \right) \\
&= \max_{\beta \in \mathbb{R}^3} (2(\beta, \xi)_{\mathbb{R}^3} - (B^*\beta, \beta)_{\mathbb{R}^3}) = ((B^*)^{-1}\xi, \xi)_{\mathbb{R}^3}.
\end{aligned}$$

Thus we have $(B^*)^{-1} = A^*$. Let us assume that the minimum in (1) is achieved for $u = u_\xi \in U$. We prove that w_1 defined by (16) is in W . Indeed, $w_1 = A\xi + A\nabla u_\xi - A^*\xi$ is in H and for any $\phi \in U$

$$\int_Y w_1 \cdot \nabla \phi dx = \int_Y (A\xi + A\nabla u_\xi - A^*\xi) \cdot \nabla \phi dx = \int_Y (A\xi + A\nabla u_\xi) \cdot \nabla \phi dx = 0,$$

where the last equality follows from (13). Thus $w_1 \in W$. By (1) and (14) for any $\mu \in \mathbb{R}^3$ we obtain

$$\begin{aligned}
\int_Y (w_1, \mu)_{\mathbb{R}^3} dx &= \int_Y (A(\xi + \nabla u_\xi), \mu)_{\mathbb{R}^3} dx - |Y| (A^*\xi, \mu)_{\mathbb{R}^3} \\
&= \int_Y (A(\xi + \nabla u_\xi), \mu)_{\mathbb{R}^3} dx - \int_Y (A(\xi + \nabla u_\xi), \mu)_{\mathbb{R}^3} dx = 0.
\end{aligned}$$

Thus $w_1 \in W_0$. Recalling that $\alpha = A^*\xi$ and the minimizing property of $u = u_\xi$ in (1) we have

$$\begin{aligned}
 (B^* \alpha, \alpha)_{\mathbb{R}^3} &= (A^* \xi, \xi)_{\mathbb{R}^3} = \frac{1}{|Y|} \int_Y (A(\xi + \nabla u_\xi), \xi + \nabla u_\xi)_{\mathbb{R}^3} dx \\
 &= \frac{1}{|Y|} \int_Y (A^{-1}(A\xi + A\nabla u_\xi), A\xi + A\nabla u_\xi)_{\mathbb{R}^3} dx \\
 &= \frac{1}{|Y|} \int_Y (A^{-1}(\alpha + w_1), \alpha + w_1)_{\mathbb{R}^3} dx.
 \end{aligned}$$

Since the minimizing field w_α is unique, we get $w_1 = w_\alpha$. □